OPTIMIZATION OF TUMOR ABLATION BY MONITORING TISSUE TEMPERATURE VIA CT

Ganga Dhar Pandeya

Ganga Dhar Pandeya
Optimization of tumor ablation by monitoring tissue temperature via CT
PhD thesis with a summary in Dutch

ISBN: 978-90-367-5718-8

Cover Image: Front cover contains three schematic pictures of ablation procedure and temperature profile at the ablation source and a CT system. Back cover contains four Mandalas.

Cover Design and Layout: GD Pandeya and MJW Greuter
Printed by: Wöhrmann Print Service - Zutphen

The work presented in this thesis was conducted at the Department of Radiology, University Medical Center Groningen, University of Groningen, The Netherlands in close collaboration with the Department of CT Engineering, Siemens AG – Healthcare Sector, Germany. Financial support for the studies described in this thesis by the Siemens AG – Healthcare, Germany is gratefully acknowledged.

The printing of this thesis was kindly supported by the University of Groningen.

rijksuniversiteit groningen

OPTIMIZATION OF TUMOR ABLATION BY MONITORING TISSUE TEMPERATURE VIA CT

Proefschrift

ter verkrijging van het doctoraat in de
Medische Wetenschappen
aan de Rijksuniversiteit Groningen
op gezag van de
Rector Magnificus, dr. E. Sterken,
in het openbaar te verdedigen op
maandag 5 november 2012
om 12.45 uur

door

Ganga Dhar Pandeya

geboren op 21 november 1974
te Harmichaur – Gulmi, Nepal

Promotor:	Prof. dr. M. Oudkerk
Copromotor:	Dr. M.J.W. Greuter
Beoordelingscommissie:	Prof. dr. J.E. Wildberger Prof. dr. ir. C.H. Slump Prof. dr. E.J. van der Jagt

Paranimfen: Hildebrand Dijkstra

Chanda Karki

Contents

CHAPTER 1

Introduction

Thermal ablation aims for coagulation of solid malignant tumors by causing direct cell destruction. As a result of the relatively high number of unresectable tumor cases and recent advances in imaging systems and interventional techniques, image guided thermal ablation has received much attention for the treatment of solid malignant tumors [1-10]. Efforts to generate specific interactions with tumor tissue in a safe and reproducible manner have recently been restricted by the unavailability of controllable energy sources, accurate monitoring systems, and problems and complications in treating specific organs. The energy sources (radiofrequency (RF), microwave, laser, etc.) have recently been refined and further customized to meet the evolving requirements for tumor treatment. In order to monitor the temperatures of tissue during ablation noninvasively, various imaging system such as ultrasound [11], magnetic resonance imaging (MRI) [12, 13] and microwave [14] are under investigation. Although current computed tomography (CT) is offering sub-second scan time, thin slice widths and high spatial and temporal resolution, it has not been explored for thermometry during thermal ablation. In this thesis the feasibility of CT thermometry during ablation of the liver tumor will be studied.

Liver Tumor

Hepatocellular carcinoma (HCC) is the most common liver tumor worldwide. The HCC incidence increased continuously in recent years and has reached 4.9 cases per 100,000 in the US [15]. Much of this increase is related to increasing incidence of hepatitis C and hepatitis B virus infections. Other risk factors for HCC include alcoholic cirrhosis, cirrhosis from hemochromatosis, primary biliary cirrhosis, and exposure to aflatoxins in parts of the world where

these are ingested [16]. Steatohepatitis has become recognized as a risk factor for cirrhosis, and HCC has been found in patients with nonalcoholic fatty liver disease. The association of diabetes with nonalcoholic fatty liver and increased risk of HCC has also been acknowledged [17].

Surgical resection or transplantation was considered as the gold standard for treatment of hepatocellular carcinoma (HCC). The overall resectability rate for such lesions is very low due to a combination of underlying chronic liver disease, lesion location and the multifocal nature of HCC. Similarly, surgical resection carries a significant associated morbidity and mortality, as well as a disease recurrence rate of up to 75% [18, 19]. Local thermal ablative techniques have gained popularity over the last decade proving to be an effective and safe alternative in many patients. These techniques are also cost effective in comparison to other treatments and are able to maximize the preservation of surrounding liver parenchyma while minimizing in-patient hospitalization [20].

Ablation Techniques

Ablation techniques use energy sources that destroy a tumor by thermal energy, with either heat (eg, RF, laser) or cold (cryoablation). Techniques for generating high tissue temperature include RF ablation [21, 22], laser ablation [23], microwave ablation [24] and high intensity focused ultrasound [25]. The energy transfer at the applicator-tissue interface is dependent on the technique used [26]. Thermal coagulation necrosis occurs when tissue is exposed to a temperature of 55–57°C [27, 28]. Thermal ablation is considered a potentially curative therapy for non-resectable hepatic malignant tumors, and should be used in accordance with established

oncological criteria for surgical treatment of malignant liver tumors regarding treatment margins [29], i.e., destruction of the targeted tumor and a 0.5 – 1cm safety margin of the surrounding hepatic parenchyma [30]. Consequently, the entire tumor and safety margin must be exposed to temperatures producing thermal coagulation necrosis. Large coagulations with predictable volume and geometry are preferable to avoid residual foci of untreated tumor. However, the rapid decay of energy with increasing distance from the energy source constrains the extent of the thermal necrosis, and restricts the clinical use of these techniques to treatment of tumors more than 3 to 4 cm in diameter. In the present study, a hot air tube, RF and a laser were used as a heat energy source to ablate liver tissue. A brief synopsis of RF and laser ablation will be provided.

RF ablation has been evaluated most extensively of the currently available ablation techniques. In monopolar systems, an electrical circuit is applied between the RF applicator and up to four neutral pads attached to the patient's skin [31]. In bipolar systems, a noninsulated electrode tip and a neutral electrode are located on the same needle shaft [32]. The principle of RF ablation results from an ionic agitation locally produced in the tissue around a noninsulated applicator tip. During ionic agitation, the tissue ion attempts to follow the changes in the direction of the alternating current which consequently induces a focal heating [33]. In order to improve the RF ablation, a substantial step forward was achieved by internal cooling via a circulating fluid in the RF applicator and using pulsed RF ablation [26]. Apart from internal cooling or fluid perfusion, other improvements were made by using multi-applicator systems. These systems consist of multi-electrodes either with parallel (cluster) electrodes or curved radially arranged electrodes (expandable electrodes).

Laser ablation with the insertion of a light-conducting quartz fiber into the tumor was described first by Bown [34]. Although this method of energy delivery is invasive, it has the advantages that there is little back-scattering and impact loss as the light strikes the tissue, and in order to reach a specific point within an organ, the surface of the body is not heated by a thermal conduit. Laser light is produced using a neodymium yttrium aluminum garnet (Nd:YAG; wavelength 1064 nm) delivered through a quartz fiber optic with a diameter of 400 mm with diffuse light emission. Laser light is converted into heat in the target area inducing coagulative necrosis, secondary degeneration and atrophy, and tumor shrinkage with minimal damage to surrounding structures [35, 36]. The size of the heated volume depends on the laser power, the laser irradiation time, the way the laser reaches the target area and optical and thermal characteristics of the treated tissue. The clinical success of laser ablation depends on the optimal positioning of the laser applicator in the centre of the lesion, an optimal monitoring of thermal changes in the treated tissue and an exact documentation of the therapy effect and the local tumor control rate.

In addition to the minimally invasive techniques mentioned above, high-intensity focused ultrasound (HIFU) is a noninvasive technique that uses focused ultrasound to generate areas of intense heat to destroy tissue anywhere in the body without breaking the skin or performing a craniotomy. Thermal ablation of pathological tissue such as prostate, liver and brain have recently been demonstrated with this unique technique [37]. The noninvasiveness of this technique should reduce the cost of complications and morbidity. Since real-time identification of the target region and accurate control of the temperature evolution during the treatment has now become possible in particular using MRI, it is foreseeable

that combining both techniques (ablative and thermometry) such as the MR–guided focused ultrasound (MRgFUS) will prove as a substitute to surgical procedures of tumor [38]. A feasibility study to implement CT thermometry during HIFU was conducted by Jenne et al. [39] who were able to show temporal and spatial temperature development during HIFU as hypodense zones in CT images but further study in this combination of techniques was not carried out.

Thermometry

Noninvasive measurement of the temperature distribution within the body is an attractive concept with the potential to visualize the three-dimensional temperature distribution created during ablation. Several methods may/can measure temperature noninvasively using MRI [12, 13], ultrasound [11], microwave [14] and CT [40, 41]. No single method can fully satisfy all requirements for effective noninvasive thermometry using current imaging systems. CT has been explored extensively for noninvasive thermometry through this study. Although CT can meet most of the above requirements, it suffers from additional issues such as metal artifacts and radiation dose.

The ideal requirements for noninvasive thermometry depend on the clinical application of the thermal therapy [42] Table 1 shows the current requirements from interventional radiologists to implement the noninvasive thermometry during thermal ablation in clinical practices.

Temperature accuracy	<1–2°C
Spatial resolution	<1–2 mm
Acquisition time	<10–30 seconds
Three-dimensional visualization	
Measurements presented in real time	
Insensitive to motion artifacts	
Compatible with medical equipment	
Low cost	

Table 1. Requirements for noninvasive thermometry

Most of the imaging systems estimate temperature by weighing the changes in repeated scans of the region of interest and are, therefore, susceptible to motion artifacts caused by deformation of liver and intra-scan and inter-scan displacement. Motion artifacts can be reduced by rapid image acquisition and breath-holding. Against other imaging systems, current CT offers a protocol with sub-second image acquisition and sub-millimeter spatial resolution. This protocol is suited for real time temperature measurement without delays between action and display, including 3D-visualisation. In addition, CT is a more widely accessible imaging system at a lower cost compared to the other imaging systems. An electromagnetic noise generated during RF ablation might interfere with the acquisition signals in MR imaging and may deteriorate image quality. Although it has been shown that a temperature accuracy of approximately 5^{o}C is feasible with the current CT system [43], criteria for temperature accuracy were not yet met. So, all the ideal requirements except for the temperature accuracy are met by current CT system, and further investigation is needed to meet that criterion as well.

Although a temperature range of 50 – 60°C is needed to assess the

extent of thermal necrosis, a wide temperature range in the tissue arises during thermal ablation with temperatures well above 100°C. Monitoring of rapidly varying temperature gradients within a small tissue volume over a 10 – 20 minutes course of treatment requires excellent spatial and temporal resolution.

CT numbers as intensity values in each pixel of CT images are proportional to electron density. The electron density is proportional to tissue type and temperature. An equation is derived to relate temperature with the change in CT number as a function of temperature T.

$$H(T) = \frac{H(T_o) + 1000}{1 + \alpha \Delta T} - 1000 \qquad \text{(eq 1)}$$

where H (T) and $H(T_o)$ are the CT number at any temperature T and at zero degrees temperature T_o, ΔT is the change in temperature and α is the thermal expansion coefficient.

This equation shows that a variation in CT number is mainly dependent on the thermal expansion coefficient

$$\alpha = -(1/\varrho).\delta\varrho/\delta T, \qquad \text{(eq 2)}$$

where ϱ is the density, $\delta\varrho$ is the change in density and δT is the change in temperature. In this equation, the thermal expansion coefficient of tissues varies consistently with temperature.

Objective and Clinical Relevance

Thermal ablation techniques, in combination with different imaging methods, have recently been described as minimally invasive strategies for the local treatment of malignant tumors [3 – 6, 44, 45]. All these ablation techniques are hampered by limited spatial and temporal information of the temperature distribution around the ablation needle and consequently on thermal dose during the

thermal ablation [42, 44]. Although with thermal ablation (and in particular RF ablation) one is able to destroy the majority of tumor cells, tumor recurrence has been reported in many cases due to the incomplete elimination of all the cancer cells. Factors such as tissue composition and peripheral cooling of the tumor by blood flow limit the volume of ablation, which may in turn lead to local tumor recurrence at the distal ablation boundary and may lead to a need for adjuvant chemotherapeutic treatments [46 – 50]. Incomplete tumor treatments are responsible for most of the tumor recurrences. Thus, a real time map of the temperature distribution may help to achieve complete tumor ablation and spare vital structures. In addition, a real time temperature map can improve the efficiency of thermal ablation and contribute to lessen the recurrence rate of tumors after ablation. The current research addresses this potential shortcoming with the development of a color coded thermal map for use in hepatic tumor treatment by means of thermal ablation. Furthermore, a thermal map may be used to calculate the cumulative equivalent minute (CEM, an equivalent minutes at 43^{o}C calculated from time-temperature history of thermal dose) during low heating thermal therapy such as hyperthermia [51].

CT has shown vast differentiation between soft and hard matter (tissue and bone). It has also the ability to distinguish between different types of soft tissues. Very few experimental studies have been done to explore the abilities of CT for thermometry in soft tissue and tumors but were not investigated well enough to adopt it yet in clinical practice. This study is intended to explore the possibility of using CT scanners to obtain the real-time temperature distribution noninvasively and finally to apply this method for the treatment of hepatic tumor using ablation technique in clinical settings.

Outline

The CT numbers are proportional to the fractional difference in effective local electron density of the subject material. Any temperature variation (spatial or temporal) in the subject material scanned will generate a CT-number shift in the CT image because of density changes due to thermal expansion. Despite very few assessment studies [39 – 41, 43, 52 – 54] for the thermal shift of CT number in various materials using early stage of CT system, no study has been presented on the thermal sensitivity of CT during heat application in liver tissue in an ex-vivo and in-vivo animal setting using current CT systems. The present study will assess the feasibility of CT thermometry. **Chapter 1** (current chapter) gives the introduction and background of this thesis.

In **chapter 2**, the first basic concept of thermal shift of CT numbers is tested in a homogeneous water sample and in inhomogeneous swine liver tissue. In **chapter 3** a study is described in which the relationship between CT value and temperature is assessed. Bovine liver tissue was heated using a multi-tined RF ablation needle in the experiments in **chapter 4**. Since various experiments verified the dependency of CT number with temperature change, **chapter 5** gives details of an in-vivo study in a swine model. Ablation was performed in liver using an RF ablation needle and the temperature was measured using fiber optical thermal sensors. A continuous laser source was used for ablation in the experiments described in **chapter 6**. Finally, all results of this study are summarized in **chapter 7**. This chapter also includes a general discussions and future perspectives.

References

1. Goldberg SN, Dupuy DE. Image-guided radiofrequency tumor ablation: challenges and oppurtunities. J vasc Interv Radiol 2001; 12:1021-1032.
2. Bischof JC, Mahr B, Choi JH, et al. Use of X-ray tomography to map crystalline and amorphous phases in frozen biomaterials. Ann of Biomed Eng 2007; 35:292-304.
3. Weld KJ, Landman J. Comparison of cryoablation, radiofrequency ablation and high-intensity focused ultrasound for treating small renal tumors. BJU Int 2005; 96:1224-1229.
4. Cheng HM, Haider MA, Dill-Macky MJ, et al. MRI and contrast-enhanced ultrasound monitoring of prostate microwave focal thermal therapy: an in vivo canine study. J of Magnetic Resonance 2008; 28:136-143.
5. Pacella CM, Bizzari G, Magnolfi F, et al. Laser thermal ablation in the treatment of small hepatocellular carcinoma: Results in 74 patients. Radiology 2001; 221:712-720.
6. Stauffer PR, Goldberg SN. Introduction: thermal ablation therapy. Int J Hyperthermia 2004; 20:671-677.
7. Becker GJ. 2000 RSNA annual oration in diagnostic radiology: the future of interventional radiology. Radiology 2001; 220: 281-292.
8. Ray Jr CE. Interventional radiology in cancer patients. Am Fam Physician 2000; 62:95-102.
9. Vogl TJ, Muller PK, Mack MG, et al. Liver metastases: interventional therapeutic techniques and results. Eur Radiol 1999; 9:675-684.
10. Montgomery ML, Sullivan JP. Advances in interventional radiology. The search for less invasive management sparks new approaches. Postgrad Med 2001; 109:93–104.
11. Seip R, Ebbini ES. Noninvasive estimation of tissues temperature response to heating fields using diagnostic ultrasound. IEEE Trans Biomed Eng 1995; 42(8).
12. Weidensteiner C, Quesson B, Caire-gana B, et al. Real time MR temperature mapping of rabbit liver in vivo during thermal ablation. Magn Reson Med 2003; 50:322-330.
13. Lepetit-Coiffe M, Quesson B, Seror O, et al. Real time monitoring of radiofrequency ablation of rabbit liver by respiratory gated quantitative temperature MRI. J Magn Reson Imaging 2006; 24:152-159.

14. Wang SS, vanderbrink BA, Regan J, et al. Microwave radiometric thermometry andits potential applicability to ablative therapy. J Interv Card Electrophysiol 2000; 4: 295-300.
15. Altekruse SF, mcglynn KA, Reichman ME. Hepatocellular carcinoma incidence, mortality, and survival trends in the United States from 1975 to 2005. J Clin Oncol 2009; 27:1485-1491.
16. Bruix J, Sherman M. Management of hepatocellular carcinoma. Hepatology 2005; 42:1208-1236.
17. Adami HO, Chow WH, Nyren O, et al.. Excess risk of primary liver cancer in patients with diabetes mellitus. J Natl Cancer Inst 1996; 88:1472-1477.
18. Zhao WH, Ma ZM, Zhou XR, Feng YZ, Fang BS. Prediction of recurrence and prognosis in patients with hepatocellular carcinoma after resection by use of CLIP score. World J Gastroenterol 2002; 8: 237-242.
19. Llovet JM, Fuster J, Bruix J. Intention-to-treat analysis of surgical treatment for early hepatocellular carcinoma: resection versus transplantation. Hepatology 1999; 30: 1434-1440.
20. Llovet JM, Mas X, Aponte JJ, et al. Cost effectiveness of adjuvant therapy for hepatocellular carcinoma during the waiting list for liver transplantation. Gut 2002; 50:123-128.
21. Dupuy DE, Liu D, Hartfeil D, et al. Percutaneous radiofrequency ablation of painful osseous metastases: a multicenter American College of Radiology Imaging Network trial. Cancer. 2010; 116:989-997.
22. Pereira PL Actual role of radiofrequency ablation of liver metastases. Eur Radiol. 2007; 17:2062-2070.
23. Vogl TJ, Straub R, Eichler K, et al. Colorectal carcinoma metastases in liver: laser-induced interstitial thermotherapy—local tumor control rate and survival data. Radiology 2004; 230:450-458.
24. Bhardwaj N, Strickland AD, Ahmad F, et al. Microwave ablation for unresectable hepatic tumours: clinical results using a novel microwave probe and generator. Eur J Surg Oncol 2010; 36:264-268.
25. Park MY, Jung SE, Cho SH, et al. Preliminary experience using high intensity focused ultrasound for treating liver metastasis from colon and stomach cancer. Int J Hyperthermia. 2009; 25:180-188.
26. Goldberg SN, Grassi CJ, Cardella JF, et al. Image-guided tumor ablation: standardization of terminology and reporting criteria. J Vasc Interv Radiol 2009; 20:S377-390.

27. Storm FK, Harrison WH, Elliott RS, Morton DL. Hyperthermic therapy for human neoplasms: thermal death time. Cancer 1980;46:1849-1854.
28. Goldberg SN, Gazelle GS, Mueller PR. Thermal ablation therapy for focal malignancy: a unified approach to underlying principles, techniques, and diagnostic imaging guidance. AJR Am J Roentgenol 2000; 174:323-331.
29. Cady B, Jenkins RL, Steele GD, Jr., Lewis WD, et al. Surgical margin in hepatic resection for colorectal metastasis: a critical and improvable determinant of outcome. Ann Surg 1998; 227:566-571.
30. Rhim H, Goldberg SN, Dodd GD 3rd, et al. Essential techniques for successful radio-frequency thermal Ablation of malignant hepatic tumors. Radiographics 2001; 21:S17-35.
31. Pereira PL, Trübenbach J, Schenk M et al. Radiofrequency ablation: In vivo comparison of four commercially available devices in pig livers. Radiology 2004; 232:482-490.
32. Burdio F, Navarro A, Sousa R et al. Evolving technology in bipolar perfused radiofrequency ablation: Assessment Of efficacy, predictability and safety in a pig liver model. Eur Radiol 2006; 16:1826-1834.
33. Organ LW. Electrophysiologic principles of radiofrequency lesion making. Appl Neurophysiol 1976; 39:69-76.
34. Bown SG. Phototherapy of tumors. World J Surg 1983; 7:700-709.
35. Beuthan J, Müller G, Schaldach B, Zur CH. Fiber designfor interstitial laser treatment. SPIE 1991; 1420: 234-241.
36. Roggan A, Müller G (1992) Computer simulations for the irradiation planning of LITT. Minim Invasive Med Tech 4:18-24.
37. Hokland SL, Pedersen M, Salomir R, et al. MRI Guided focused ultrasound: methodology and applications. IEEE Trans Med Imaging 2006; 25:723-731.
38. Bradley WG Jr. MR-guided focused ultrasound: A potentially disruptive technology. J Am Coll Radiol 2009; 6:510 – 513.
39. Jenne JW, Bahner M, Spoo J, Huber P, Rastert R. CT on-line monitoring of HIFU therapy. IEEE Ultrasonics Symposium 1997; 1377-1380.
40. Pandeya GD, Greuter MJW, de Jong KP, Schmidt, et al. Feasibility of noninvasive temperature assessment during radiofrequency liver ablation on computed tomography. J Comput Assist Tomogr 2011; 35:356-360.
41. Pandeya GD, Klaessens JHGM, Greuter MJW, et al. Feasibility of Computed Tomography based thermometry during interstitial laser heating in bovine liver. Eur Radiol 2011; 8: 1733-1738.

42. Frich, L. Non-invasive thermometry for monitoring hepatic radiofrequency ablation. Minim Invasiv Ther 2006; 1:18-25.
43. Bruners P, Levit E, Penzkofer T, et al. Multi-slice computed tomography: A tool for non-invasive temperature measurement? Int J Hyperthermia 2010; 26:359-365.
44. Goldberg SN, Dupuy DE. Image-guided radiofrequency tumor ablation: challenges and opportunities – Part I. J vasc Interv Radiol 2001; 12:1021-1032.
45. Bischof JC, Mahr B, Choi JH, et al. Use of X-ray tomography to map crystalline and amorphous phases in frozen biomaterials. Ann of Biomed Eng 2007; 35:292-304.
46. Bartolozzi C, Crocetti L, Cioni D, et al. Assessment of therapeutic effect of liver tumor ablation procedures. Hepatogastroenterology 2001; 48:352-358.
47. Cioni D, Lencioni R, Bartolozzi C, Percutaneous ablation of liver malignancies: imaging evaluation of treatment response. Eur J Ultrasound 2001; 13:73-93.
48. Lencioni R, Goletti O, Armillotta N, et al. Radio-frequency thermal ablation of liver metastases with a cooled-tip electrode needle: results of a pilot clinical trial. Eur Radiol 1998 1205-1211.
49. Francica G, Marone G, Ultrasound-guided percutaneous treatment of hepatocellular carcinoma by radiofrequency hyperthermia with a 'cooled-tip needle'. A preliminary clinical experience. Eur. J. Ultrasound 1999; 9:145-153.
50. Buscarini L, Rossi S, Technology for radiofrequency thermal ablation of liver tumors, Semin. Laparosc Surg 1997; 4: 96-110.
51. Mertyna P, Dewhirst MW, Halpern E, et al. Radiofrequency ablation: The effect of distance and baseline temperature on thermal dose required for coagulation. Int J Hyperthermia 2008; 24:550- 559.
52. Fallone BG, Moran PR, Podgorsak EB. Noninvasive thermometry with a clinical x-ray CT scanner. Med Phys 1982;9:715-721.
53. Bentzen SM, Overgaard J, Jorgensen J. Isotherm mapping in hyperthermia using subtraction X-ray computed tomography. Radiotherapy and Oncology 1984; 2:255-260.
54. Zamenhof RG, Sternick ES, Curran BM. Non-invasive temperature mapping by computerized tomography. Int J Radiat Oncol Biol Phys 1981;7:1235.

CHAPTER 2

Assessment of thermal sensitivity of computed tomography during heating of liver: an ex-vivo study

Br J Radiol 2012; 85:e661-e665

G. D. Pandeya[1,2], M. J. W. Greuter[1], B. Schmidt[2], T. Flohr[2] and M. Oudkerk[1]

1. Department of Radiology, UMC Groningen, University of Groningen, The Netherlands

2. Computed Tomography Division, Siemens Healthcare, Forchheim, Germany

Abstract

Objectives

The purpose of this study was to assess the thermal sensitivity of computed tomography (CT) during heating of ex-vivo animal liver.

Materials and Methods

Swine liver was indirectly heated from 20°C to 90°C by passage of hot air through a plastic tube. The temperature in the heated liver was measured using calibrated thermocouples. In addition, image acquisition was performed with a multi-slice CT scanner before and during heating of the liver sample. The reconstructed CT images were then analyzed to assess the change of CT number as a function of temperature.

Results

During heating, a decrease in CT numbers was observed as a hypodense area in the CT images. In addition, the hypodense area extended outward from the heat source during heating. The analysis showed a linear decrease of CT number as a function of temperature. From this relationship we derived a thermal sensitivity of CT for swine liver tissue as -0.54±0.03 HU/°C with R-square value of 0.91.

Conclusions

The assessment of the thermal sensitivity of CT in ex-vivo swine liver tissue showed a linear dependency on temperature up to 90°C. This result may be beneficial for the application of isotherms or thermal maps in CT images of liver tissue.

Introduction

Thermal ablation therapy of liver tumors has received much attention as a minimally invasive method for local treatment of solid malignancies [1-5]. Several techniques for thermal ablation therapy [6,7] such as radiofrequency ablation (RFA), laser ablation, microwave ablation and high intensity focused ultrasound (HIFU) are in clinical practice. During thermal ablation therapy the tumor should be heated at temperatures above 56^{o}C [8] or its cumulative equivalent minute (CEM), whereas adjacent healthy tissue and blood vessels should stay below 40^{o}C. Thus, the assessment of temperature distribution during thermal ablation therapy is essential for complete tumor necrosis. In order to assess the temperature in the ablation zone, invasive interstitial thermometry can be used. However, invasive thermometry can only be performed at a limited number of points in the liver due to several complications [9,10]. Therefore, several non-invasive techniques for temperature measurement are in clinical use. Most of these non-invasive techniques are based on microwave radiometry [11], magnetic resonance imaging [12] and ultrasound imaging [14,15] but these techniques are sensitive to motion and misregistration artifacts in moving and refilling organs like kidney, liver and lungs. Alternatively, Computed Tomography (CT) gained interest by overcoming those limitations and by offering an almost real-time monitoring technique for ablation therapy [16].

A CT scanner yields CT numbers which are proportional to the fractional difference in effective local electron density of the subject material. Any temperature variation (spatial or temporal) in the subject material scanned will generate a CT-number shift in the CT image because of density changes due to thermal expansion.

Despite very few assessment studies [16-22] for the thermal shift of CT number in various material using early stage of CT system, no study have been presented on the thermal sensitivity of liver tissue during heat application using current CT system. Therefore, the purpose of this study is to assess the CT thermal sensitivity of liver tissue during heat application in an ex-vivo setting.

Materials and Methods

The study was conducted after obtaining approval from the institutional ethical committee for animal care. A liver was extracted within 12 hours after sacrifice of a swine. From the liver, three circular tissue discs that were 9 cm in diameter and approximately 5 cm thick were prepared. Each tissue disc was placed into a 9 cm internal diameter poly-methyl-meth-acrylate (PMMA) cylinder (Figure 1). The tissue disc was heated using a hot

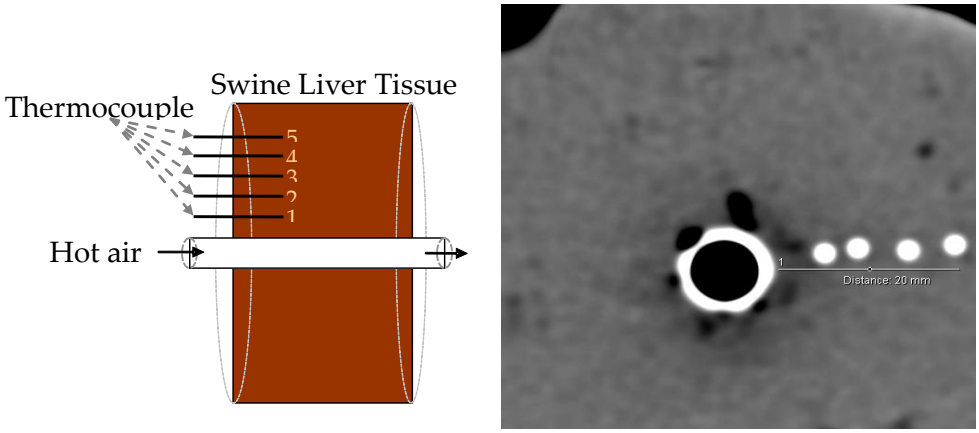

Figure 1
Schematic drawing of experimental set-up of the liver tissue in the PMMA cylinder (left) and placement of 5 thermocouples. An example of reconstructed CT image at room temperature showed the positions of thermal sensors from heating tube (right).

poly-tetra-fluoro-ethylene (PTFE) tube. The tube with a diameter of 9 mm and thickness of 2 mm was placed through the central axis of the tissue disc and fixed by centrally drilled holes in two PMMA end plates. The tube was heated from 20°C to 90°C by the flow of the hot air. The hot tube subsequently acts as a heat source. Five 1 mm diameter holes were spaced at 5, 10, 15, 20 and 25 mm distance parallel from the central axis. Five thermally insulated thermocouples (NiCr-Ni, Roessel Messtechnik, Dresden, Germany) with a diameter of 0.25 mm were inserted through these holes into the liver tissue up to a depth of 3 cm. The temperatures were recorded in a computer using a data logger (TopMessage, Delphine Technology AG, Gladbach, Germany) and its software. Thermocouple 1 was taken as a reference temperature in order to assess the temperature during heating. However, for the calculation, the reading from all thermocouples and respective variation in CT numbers were used.

The liver tissue was scanned using a multi-detector CT (Somatom Definition, Siemens AG - Healthcare, Germany) in sequential acquisition mode (pitch = 1) with 120 kVp, 200 mAs, 24x1.2 mm collimation and 500 ms rotation time. CT images were reconstructed at a slice thickness of 1.2 mm using a B31s kernel on a dedicated workstation (Syngo, Siemens AG - Healthcare, Germany). At least one scan before heating and 5 scans during heating in each examination were performed. The radiation dose (CTDIvol) and dose-length product (DLP) during each examination was read from the workstation of the CT system. The effective dose per CT examination was calculated using a DLP-to-effective dose conversion factor for the liver of 0.015 [23].

In the reconstructed CT images, a circular region of interest (ROI) of

approximately 21 mm^2 was manually drawn covering the tip of the thermocouples in one experiment. The CT number histogram was calculated for each ROI. From each histogram, lower and upper Hounsfield unit thresholds were determined to include only pixels belonging to tissue (Figure 2) for further calculations. The ROI was drawn at the tip of the thermocouples in all experiments. Using average upper and lower thresholds, the mean CT number and standard deviation were calculated in all ROIs for all 40 measurements. The standard deviation in the average CT number in the ROI in each examination was used to quantify noise. The measured data were analysed using statistical software (SPSS 16.0, SPSS Inc, Chicago, USA). The accuracy of the fit was determined by calculating the Pearson correlation coefficient (r^2).

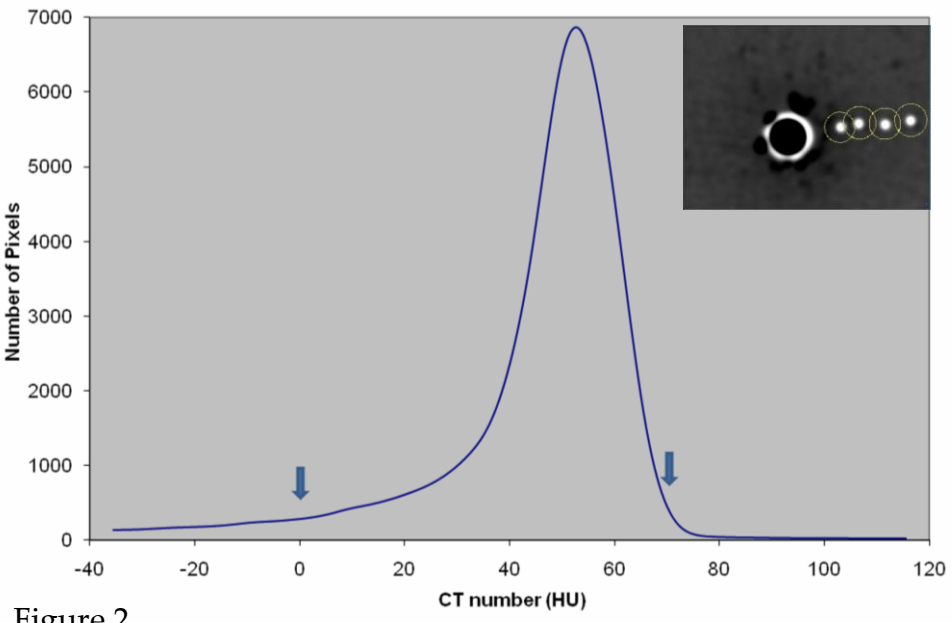

Figure 2

Example of histogram used to compute the upper and lower threshold to mask voxels of non-tissue structure from the measurements. The lower and upper thresholds were shown by arrows at 0 HU and 70 HU.

Results

The temperature in the tissue rose from room temperature (17°C) up to 90°C as recorded by thermocouple 1 (Figure 1) and at the same time, the temperature recorded by the other four thermocouples declined at increasing distance from the heat source.

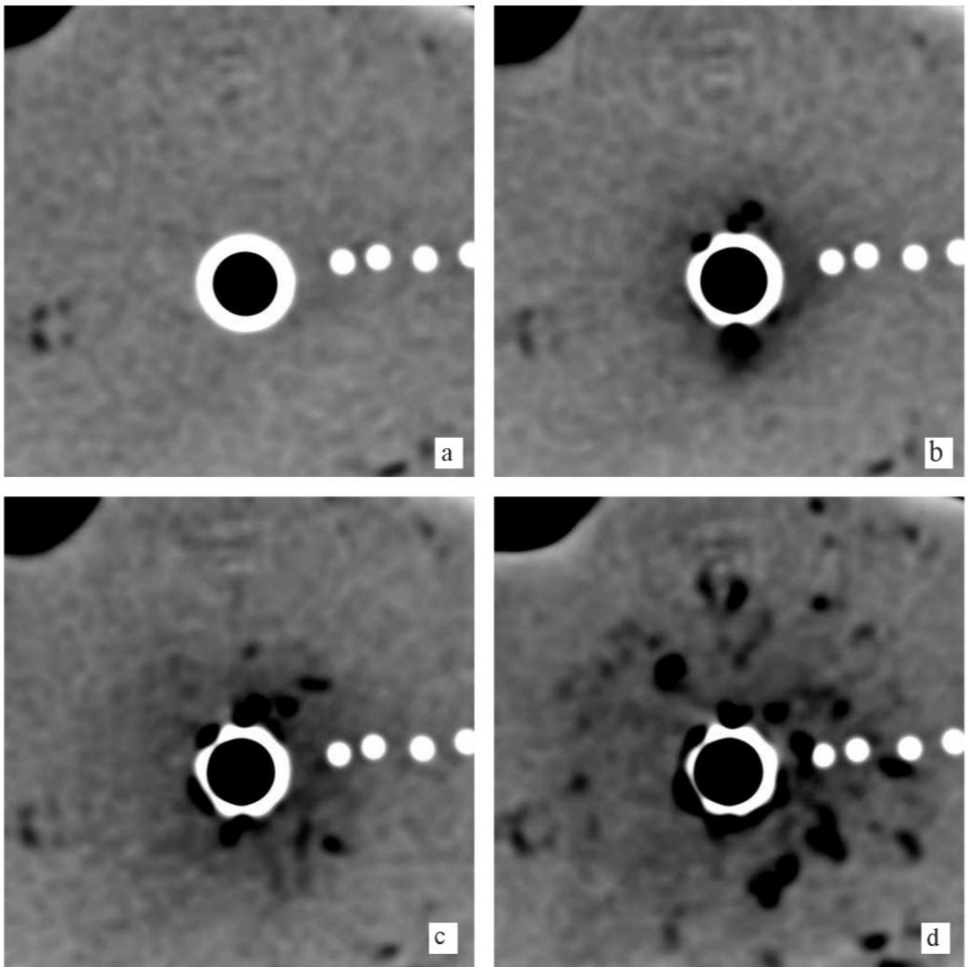

Figure 3
Example of CT images at temperatures a) 20°C, b) 40°C, c) 60°C and d) 80°C as measured by thermocouple 1. The images showed a hypodense area around the heat source which was increased at increasing temperature.

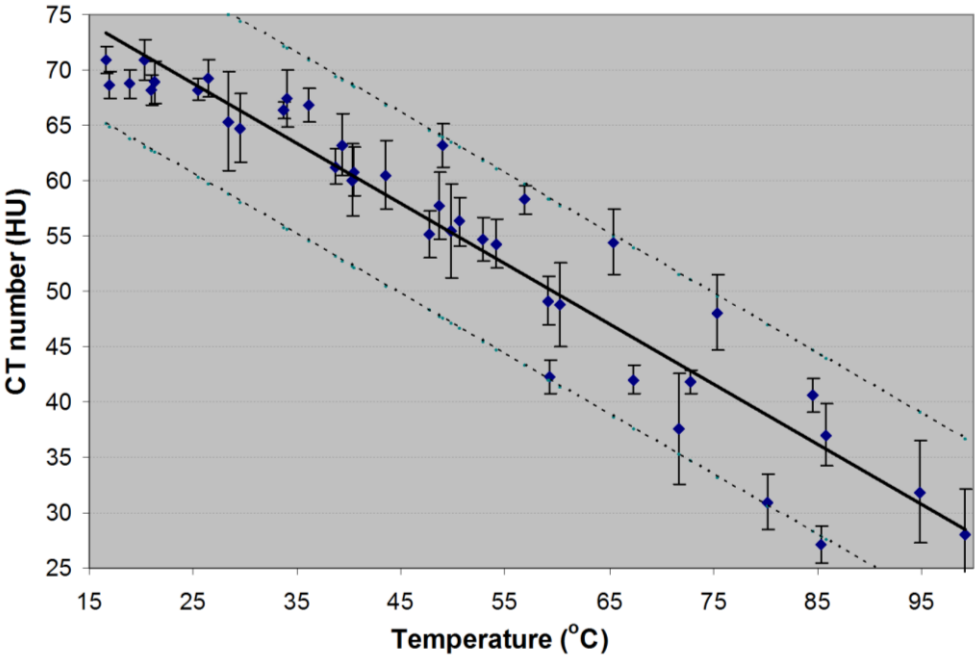

Figure 4

CT number as a function of temperature in liver tissue during heating. The solid line represents a least-square linear fit with R^2=0.91. The dotted line represents the 95% predication interval (PI). Most of the data (~98%) fell within the PI.

Figure 3 shows the CT images of liver tissue at room temperature (20°C) (Figure 3a) to 80°C (Figure 3d) measured by thermocouple 1 (Figure 1). A decrease in CT numbers as a hypodense area due to increase in heating was observed (Figure 3). In addition, the extent of hypodense area increased during heating. Gas pockets were formed nearer to the hot tube at the beginning of the heating process and continued to develop at larger distances from the hot tube at increased temperatures.

From the histogram analysis we derived the lower and upper thresholds at 0±4.9 HU and 70±6.8 HU respectively (Figure 2). The noise increased with temperature from 2 HU at 17°C to 14 HU at

90°C. The CTDIvol was 277 mGy corresponding to a DLP of 798 mGycm. Using the DLP-to-effective dose conversion factor this corresponds to an effective dose of approximately 12 mSv.

The linear decline of CT numbers as a function of temperatures is shown in Figure 4. In graph, 98% of the data falls within the 95% prediction interval. Only one set of data points as an outlier was observed at approximately 85°C. A CT thermal sensitivity of -0.54±0.03 HU/°C (r^2=0.91) was determined for the range of 20 °C - 90°C.

Discussion

We have shown that CT numbers of ex-vivo pig liver are linearly dependent on temperature with a thermal sensitivity of -0.54±0.03 HU/°C (r^2=0.91).

The need for accurate temperature assessment of the ablation zone arises from re-occurrence of tumors in the liver after thermal ablation therapy. These re-occurrences are thought to arise from inadequate temperature information of the ablation zone. Therefore, real-time information on the spatial distribution of temperature in the ablation zone would provide valuable information for more efficient ablation. Several studies have shown the influence of temperature on CT number [16-22].

The thermal sensitivity we found is significantly higher than the values reported for muscle tissue, i.e. -0.45±0.01 HU/°C and -0.43±0.03 HU/°C and also approximately 20% increased CT number with respect to these two studies [16, 20]. These differences were mainly contributed by the type of tissues and CT systems used in the studies.

Criteria for non-invasive thermometry for the monitoring of thermal ablation are: a spatial resolution better than 2 mm (1), an acquisition time less than 30 s (2) and temperature accuracy in the order of 1 – 2°C (3) [24]. In the present study criteria (1) and (2) were met with a spatial resolution of 1.2 mm and an acquisition time of 500 ms. Although it has been shown that a temperature accuracy of approximately 5°C is feasible with sub-millimeter spatial resolution [19], criterion (3) was not met. The temperature accuracy can be increased by improving the CT image quality and using non-metallic thermal sensors.

For CT temperature assessment, it is necessary to perform a baseline scan and at least 6 repeated scans to monitor the temperature induced changes in CT numbers [19]. For the treatment of a single hepatic tumor of 30 mm, approximately 50 mm should be covered during the CT scan to include a safety margin. During the positioning of the heat source or RF needle in the liver, a low dose CT protocol can be used like CT fluoroscopy. However, this protocol cannot be used for monitoring of the temperature distribution because of poor image quality.

We derived an effective dose of approximately 12 mSv for the entire ablation procedure using CT temperature assessment. If the procedure would have been done without CT temperature assessment, the effective dose would have been approximately 2 to 4 mSv depending on the specific CT technique used. This implies that CT temperature assessment technique adds an excess effective dose for the patient of 8 to 10 mSv. Using a tumor induction probability of 5% per Sv, this excess effective dose would yield 1 extra fatal tumor in 2000 to 2500 patients. However, this number has to be compared to the number of patients which do not suffer

from local recurrences or distant metastasis because of incomplete tumor ablation without CT temperature assessment. Although we have no information about the actual skin dose, it is highly unlikely that this effective dose of 12 mSv would yield a skin dose which lies in the range of skin erythema (i.e. 200 cGy). During in-vivo implementation of this method, one may need additional scans in order to follow the heating pattern accurately and to assess the cooling effects due to blood perfusion. The excess effective dose delivered to the patient can be further reduced by limiting the number of scans and by optimizing imaging technique to monitor the heating pattern.

This study was performed in ex-vivo liver tissue and further animal studies are essential to understand the vascular and perfusion response to heating. The interpretation of vascular and perfusion response during heating is very difficult due to complex morphology of living tissue [25]. Heating causes initial vasodilatation but at higher temperature vasoconstriction occurs and as a consequence the tissue blood volume changes and as an additional consequence the heat distribution. Highly perfused tissue with large vessels may act as a heat sink by transporting heat from the local tissue to the peripheral tissue [26-28]. The effect of perfusion makes native liver parenchyma relatively more resilient to thermal damage than tumour tissue. This effect can cause a more asymmetric temperature distribution and a more irregular necrosis zone [29] than the approximately radial symmetric temperature distribution shown in the present study. To implement this method into further animal studies, the role of vascular and perfusion should be correctly interpreted.

With the use of temperature sensitivity derived in this study, the

CT images can be used to transform temperature distribution into a color coded map. Furthermore, temperature information could be used in low heating therapy like hyperthermia to calculate cumulative equivalent minute (CEM) or thermal dose.

There are certain limitations in this study. First, the lack of surrounding saline or agar to mimic a body could have influenced CT numbers and image noise particularly at the border of the liver tissue. However this had a minor influence in the local heated area. Secondly, it had been supposed that thermally ablated tissue may actually increase in CT number, due to phase transitions in tissue, especially at coagulation by changing tissue density. Such tissue characteristics due to desiccation were not observed during heating but it could be seen when tissue cools down. Although, the main concerned of this study is to determine the area of necrosis by detecting the region with temperature > 60^{o}C [30] during heating, further study may be necessary to investigate the increase in CT number during cooling. Finally, this study does not resemble an in-vivo situation where additional physiological processes and inhomogeneous structures increase the CT noise [31]. Therefore further studies using CT for the noninvasive temperature assessment are needed to verify the current results in an in-vivo situation.

In this study, the non-invasive approach of current CT system was assessed for temperature discrimination during tissue heating. The method presented here could be used to assess non-invasive CT temperature mapping in an in-vivo study.

References

1. Abitabile P, Hartl U, Lange J, Maurer CA. Radiofrequency ablation permits an effective treatment for colorectal liver metastasis. Eur J Surg Oncol 2007; 33:67-71.
2. Allgaier HP, Deibert P, Zuber I, et al. Percutaneous radiofrequency interstitial thermal ablation of small hepatocellular carcinoma. Lancet 1999; 353:1676-1677.
3. Amersi FF, McElrath-Garza A, Ahmad A, et al. Long-term survival after radiofrequency ablation of complex unresectable liver tumors. Arch Surg 2006; 141:581-588.
4. Thanos L, Mylona S, Galani P, et al. Overcoming the heat-sink phenomenon: successful radiofrequency thermal ablation of liver tumors in contact with blood vessels. Diagn Interv Radiol 2008; 14:51-56.
5. Park BJ, Byun JH, Jin YH, et al. CT-guided radiofrequency ablation for hepatocellular carcinomas that were undetectable at US: Therapeutic effectiveness and safety. J Vasc Interv Radiol 2009; 20:490-499.
6. Mertyna P, Goldberg W, Yang W, Goldberg SN. Thermal ablation a comparison of thermal dose required for radiofrequency-, microwave-, and laser- induced coagulation in an ex-vivo bovine liver model. Acad Radiol 2009; 16:1539-1548.
7. Weld KJ, Landman J. Comparison of cryoablation, radiofrequency ablation and high-intensity focused ultrasound for treating small renal tumors. BJU Int 2005; 96:1224-1229.
8. Goldberg SN, Dupuy DE. Image radiofrequency tumor ablation: challenges and opportunities – part 1. J Vasc Interv Radiol 2001; 12:1021-1032.
9. Van der Zee J, Peer-Valstar JN, Rietveld PJ, et al. Practical limitation of interstitial thermometry during deep hyperthermia. Int J Radiat Oncol Biol Phys 1998; 40:1205-1212.
10. Wust P, Gellerman J, Harder C, et al. Rationale for using invasive thermometry for regional hyperthermia of pelvic tumors. Int J Radiation Oncology Biol Phys 1998; 41:1129-1137.
11. Wang SS, VanderBrink BA, Regan J, et al. Microwave radiometric thermometry andits potential applicability to ablative therapy. J Interv Card Electrophysiol 2000; 4:295-300.

12. Weidensteiner C, Quesson B, Caire – Gana B, et al. Real time MR temperature mapping of rabbit liver in vivo during thermal ablation. Mag Reson Med 2003; 50:322-330.
13. Lepetit-Coiffe M, Quesson B, Seror O, et al. Real time monitoring of radiofrequency ablation of rabbit liver by respiratory gated quantitative temperature MRI. J Mag Reson Imaging 2006; 24:152-159.
14. Arthur RM, Straube WL, Starman JD, Moros EG. Noninvasive temperature estimation based on the energy of backscattered ultrasound. Med Phys 2003; 30:1021-1029.
15. Seip R, Ebbini ES. Noninvasive estimation of tissues temperature response to heating fields using diagnostic ultrasound. IEEE Trans. Biomed. Eng 1995;42(8).
16. Fallone BG, Moran PR, Podgorsak EB. Noninvasive thermometry with a clinical x-ray CT scanner. Med Phys 1982; 9:715-721.
17. Bentzen SM, Overgaard J, Jorgensen J. Isotherm mapping in hyperthermia using subtraction X-ray computed tomography. Radiother Oncol 1984; 2:255-260.
18. Zamenhof RG, Sternick ES, Curran BM. Non-invasive temperature mapping by computerized tomography. Int J Radiat Oncol Biol Phys 1981; 7:1235.
19. Bruners P, Levit E, Penzkofer T, et al. Multi-slice computed tomography: A tool for non-invasive temperature measurement? Int J Hyperthermia 2010; 26:359-365.
20. Jenne JW, Bahner M, Spoo J, et al. CT on-line monitoring of HIFU therapy. IEEE Ultrasonics Symposium 1997;1377-1380.
21. Pandeya GD, Greuter MJW, de Jong KP, et al. Feasibility of noninvasive temperature assessment during radiofrequency liver ablation on computed tomography. J Comput Assist Tomogr 2011; 35:356-360.
22. Pandeya GD, Klaessens JHGM, Greuter MJW, et al. Feasibility of Computed Tomography based thermometry during interstitial laser heating in bovine liver. Eur Radiol 2011; 8: 1733-1738.
23. Christner JA, Kofler JM, and McCollough CH. Estimating effective dose for CT using dose-length product compared with using organ doses: consequences of adopting International Commission on Radiological Protection publication 103 or dual-energy scanning. AJR 2010; 194: 881-889.
24. Frich L. Non-invasive thermometry for monitoring hepatic radiofrequency ablation. Minim Invasive Ther 2006;15:18-25.

25. Arkin H, Xu LX, Holmes KR. Recent developments in modeling heat transfer in blood perfused tissues. IEEE Trans Biomed Eng 1994; 41:97-107.
26. Whelan WM, Wyman DR, Wilson BC. Investigations of large vessel cooling during interstitial laser heating. Med Phys 1995; 22:105-115.
27. Welp C, Siebers S, Ermert H, Werner J. Investigation of the influence of blood flow rate on large veseel cooling in hepatic radiofrequency ablation. Biomed Tech(Berlin) 2006; 51:337-346.
28. Ritz J, Lehmann KS, Isbert C, et al. In-vivo evaluation of a novel bipolar radiofrequency device for interstitial thermotherapy of liver tumor during normal and interrupted hepatic perfusion. J Surg Res 2006;133:174-184.
29. Jiang SC, Zhang XX. Dynamic modelling of photothermal interactions for laser-induced interstitial thermotherapy: parameter sensitivity analysis. Lasers Med Sci 2005; 20:122-131.
30. Goldberg SN, Gazelle GS, Halpern EF, et al. Radiofrequency tissue ablation: importance of local temperature along the electrode tip exposure in determining lesion shape and size. Acad Radiol 1996; 3:212- 218.
31. Bydder GM, Kreel L. The temperature dependence of computed tomography attenuation values. J Comput Assist Tomogr 1979; 3:506-510.

CHAPTER 3

Calibration of temperature measurements with CT for ablation of liver tissue

Proc. SPIE – Medical Imaging 2010; 7625
DOI:10.1117/12.844313

G. D. Pandeya[1,2], M. J. W. Greuter[1], B. Schmidt[2], T. Flohr[2] and M. Oudkerk[1]

1. Department of Radiology, UMC Groningen, University of Groningen, The Netherlands

2. Computed Tomography Division, Siemens Healthcare, Forchheim, Germany

Abstract

The purpose of this study was to determine the relationships between the CT value and temperature for the range of ablation therapy. Bovine liver was slowly heated and image acquisition was performed with a clinical CT. Real time temperature was measured and stored using calibrated thermal sensors. Images were analyzed at CT workstation. It was feasible to validate the spatial and temporal temperature growth during heating by means of declining CT values in the performed images. The thermal sensitivity for liver tissue was -0.54±0.10 HU/^{o}C. It is concluded that CT can be calibrated to predict temperature distribution during heating.

Introduction

During ablation therapy, tumor tissue is, preferably, heated at temperatures above 56°C [1] whereas adjacent healthy tissue and blood vessels should stay below 40°C. To asses the temperature distribution, invasive method like implanting temperature probes at the region of ablation and near to vital organ are may be traumatic for the patient [2, 3] and such methods may provide limited information. Moreover, most non-invasive systems like microwave radiometry [4], magnetic resonance imaging [5, 6] and ultrasound [7, 8], are insensitive to temperature changes in moving and refilling organs. Another novel non-invasive technique is computed tomography (CT) which might overcome the limitations faced by other techniques. The pioneering work of Fallone et al [9] (1982) demonstrated that the change in CT number in tissue can very well be correlated with temperature. Other existing literature data [7, 9, 10] also supports the concepts of non-invasive methods to obtain the temperature of tissue.

The interpretation of temperatures in CT images is not possible without knowledge of the relationship between the CT number and temperature. Such a calibration has not been reported in any previous study for the ablation of ex-vivo liver tissue. Thus, the purpose of this study is to determine the correlation between the CT number and the measured temperature during heating of ex-vivo liver tissue.

Materials and method

A bovine liver was used within 6 hours after slaughter and placed into a perspex cylinder with a diameter of 90 mm. The liver was heated using a multi-tined ablation probe (StarBurst Talon, Angiodynamics, New York USA) in combination with a radio-frequency ablation (RFA) system (Angiodynamics, New York USA). The ablation probe was inserted in the liver at the central axis of the cylinder at a depth of 50 mm as shown in figure 1. In addition, we inserted five calibrated thermocouple (NiCr-Ni) sensors of diameter 0.25mm in the liver at a depth of 53 mm and at a distance of 5, 10, 15, 20 and 25 mm respectively from the ablation probe (figure 1). During the ablation process we heated the liver from room temperature (20^{o}C) to 100^{o}C as measured by the five thermocouple sensors attached to a data logger (TopMessage, Delphine Technology, Germany). The data logger was connected to a computer which stored the measured temperatures every second.

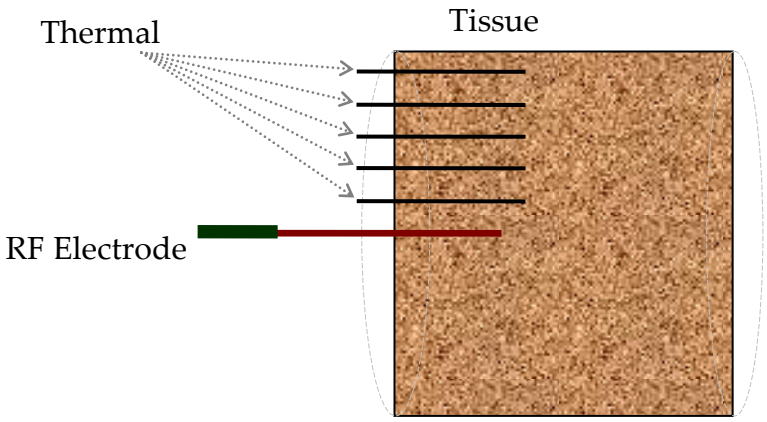

Figure 1
Experimental set up for bovine liver tissue phantom inside the cylindrical Perspex container.

The liver was scanned using a 1st generation dual source CT scanner (SOMATOM Definition, Siemens AG – Healthcare, Germany) in single source mode. All CT images were acquired in sequential mode using 120 kVp, 210 mAs, a collimation of 32 x 0.6 mm and a temporal resolution of 250 ms. The acquired images were reconstructed with a slice thickness of 5 mm and an increment of 5 mm in a field of view of 300 mm with a B31s kernel on a Syngo Acquisition Workplace (Siemens AG – Healthcare, Germany).

A circular region of interest (ROI) with an area of approximately 10 mm^2 was manually drawn within a distance of 1 mm to the tip of each of the five thermal sensors. From the ROI the mean and standard deviation of the Hounsfield units were calculated. The dependency of the CT number on temperature was fitted using a straight line: $H = a_1T + a_0$ where H, a_n and T are CT number, coefficients with n=0,1 and temperature respectively. Statistical analysis was performed using a least square fit. The goodness of the fit was tested by calculating the Pearson correlation coefficient (R^2).

Results

The CT number of the liver tissue decreased linearly as a function of temperature (fig 2). The thermal sensitivity of CT for liver tissue was -0.54±0.10HU/^oC (R^2=0.97). The calibration curves from previous studies slightly differ from our result (fig 2. Figure 3 shows examples of the ablated liver at increasing temperatures. From this figure the decrease in CT number and the heat propagation in the ablated liver can be appreciated.

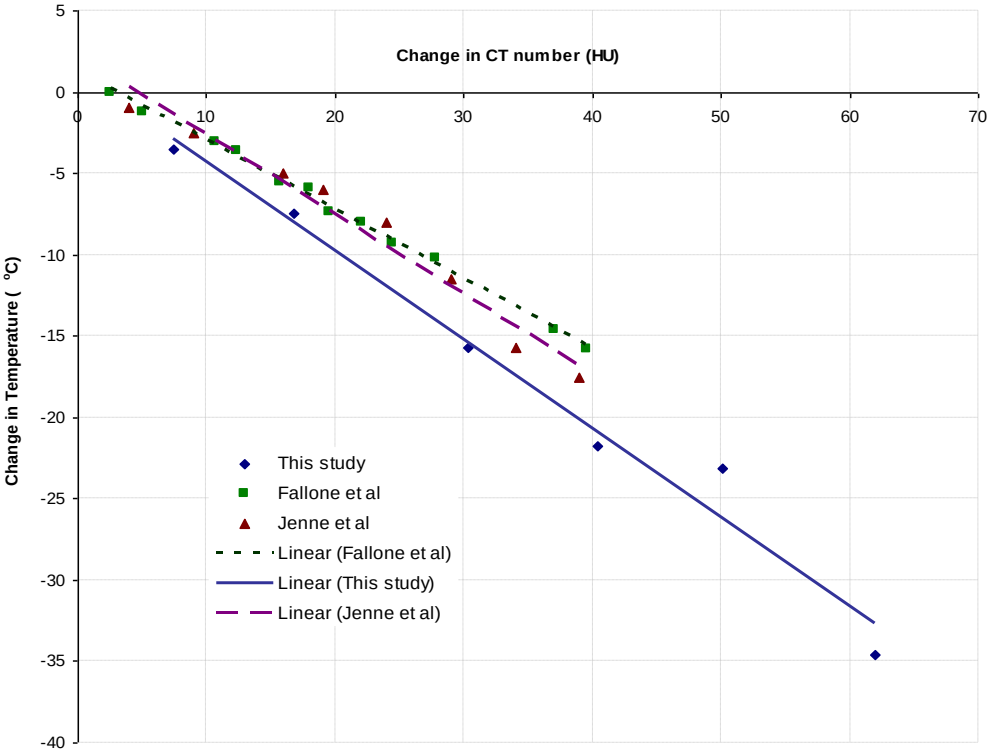

Figure 2

Change in CT number as a function of increased temperature for bovine liver tissue during ablation. The solid line represents a least-square linear fit to the all data.

Discussion

We have shown that the CT number is linearly dependent on temperature during ablation of liver tissue with a thermal sensitivity of -0.54±0.04 HU/°C. Fallone et al [9] (1982) and Jenne et al. reported a CT thermal sensitivity of -0.45 HU/°C and -0.43 HU/°C respectively. Despite the relatively larger CT numbers found in our study compared to previous studies [9, 11, 12], our study also showed a linear dependency of CT thermal sensitivity. The

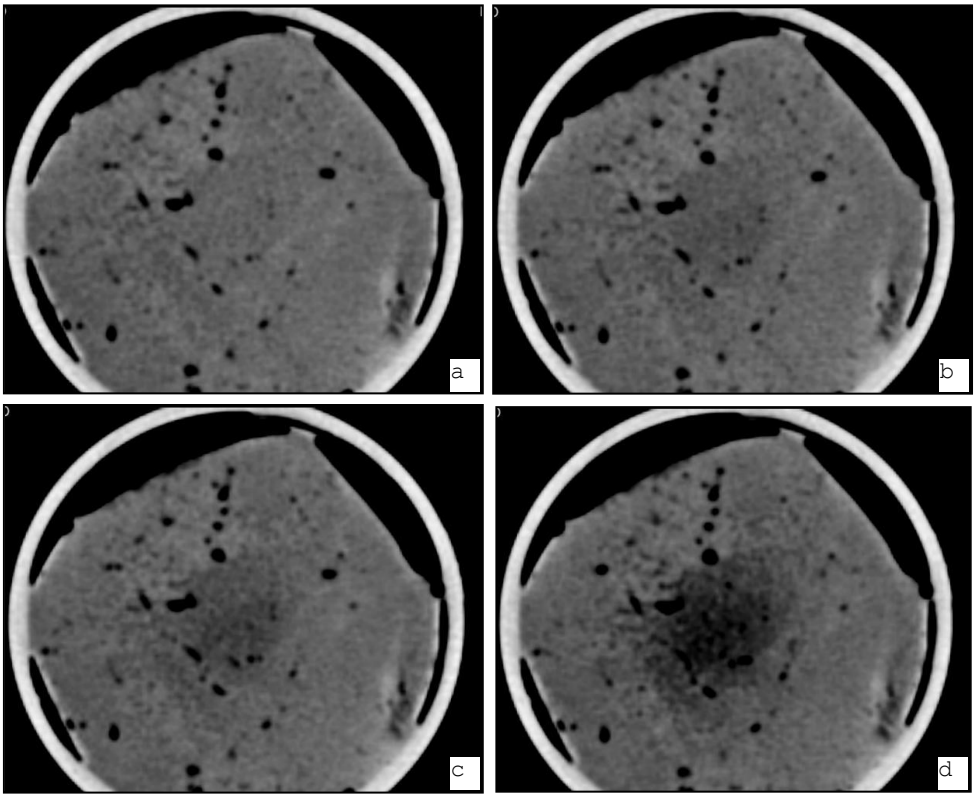

Figure 3
Original CT image with temperature 40°C, 45°C, 53°C and 60°C near the tip of RF probe measured by a thermal sensor. Series of CT scan is demonstrating declining CT number during ablation and displaying heat propagation in fresh bovine liver tissue.

differences may be caused by the improved spatial resolution of the used CT scanner. ,Previous studies [9, 10, 11] were performed with a 3rd generation CT scanner with 6 s scan time, 85mA tube current at 120 kV and 15 mm slice width wheras this calibration study has been done with sub-second scan time, thin slice width (up to 0.6mm) and high spatial as well as temporal resolution. In addition, the thermal sensitivity in previous studies was measured for a

relatively small temperature range (20-60°C) whereas in this study the thermal sensitivity was measured from 20°C to 90°C.

When tissue is exposed to a higher than physiological temperature, excessive intermolecular physical forces will be generated which leads to molecular changes and finally conducts tissue necrosis when the temperature reaches certain values. The tissue vulnerability to thermal damage depends on molecular structure and strength of bonds but not on cell size or shape. Therefore, the susceptibility to heat damage is quite similar across different tissue types [13, 14]. Even though our model validation was based on ablation of normal liver tissue, we anticipate similar results in tumor and other tissue types.

There are certain limitations in our ex-vivo study which should be considered when interpreting the results. First, the partial volume effect may give rise to unreliable CT numbers when the volume element represented by a pixel includes tissue components with highly different attenuation coefficients [15]. This effect is particularly important for the interpretation of CT numbers near the ablation electrode or near the air pocket at the ablation zone. Therefore the acquired data was reconstructed in relatively thin slices (5 mm) in order to minimize the partial volume effect [16]. Secondly, the topology of our liver phantom did not represent an in-vivo hepatic topology. Liver tissue with fewer blood vessels to minimize the formation of air pockets during heating was used in this study. Thirdly, the thermocouple might induce a heat conduction effect on the temperature distribution in our phantom. However, because very thin thermocouples (0.25 mm in diameter) were used at a relatively large distance from each other (5 mm), it is assumed that this effect does not significantly alter our results.

Fourthly, the tissue was not perfused. Since it has been shown that perivascular perfusion act as heat sink in tissue cooling by continuously transporting heat [17, 18, 19] this effect has to be considered in our results and for further study.

Conclusion

The CT number of liver tissue depends linearly on temperature during an RF ablation therapy. The outcome of this study can be used to explore the temperature distribution and for the calculation of isotherms in the CT images during ex-vivo ablation studies.

References

1. Goldberg SN and Dupuy DE. Image radiofrequency tumor ablation: challenges and opportunities – part 1. J Vasc Interv Radiol 2001; 12:1021-1032.
2. Van der Zee J, Peer-Valstar JN, Rietveld PJ, et al. Practical limitation of interstitial thermometry during deep hyperthermia. Int J Radiat Oncol Boil Phys 1998; 40:1205-1212.
3. Wust P, Gellerman J, Harder C, et al. Rationale for using invasive thermometry for regional hyperthermia of pelvic tumors. Int J Radiat Oncol Biol Phys 1998; 41:1129-1137.
4. Wang SS, VanderBrink BA, Regan J, et al. Microwave radiometric thermometry andits potential applicability to ablative therapy. J Interv Card Electrophysiol 2000; 4:295-300.
5. Weidensteiner C, Quesson B, Caire-Gana B, et al. Real time MR temperature mapping of rabbit liver in vivo during thermal ablation. Magn Reson Med 2003; 50:322-330.
6. Lepetit-Coiffe M, Quesson B, Seror O, et al. Real time monitoring of radiofrequency ablation of rabbit liver by respiratory gated quantitative temperature MRI. J Magn Reson Imaging 2006; 24:152-159.
7. Arthur RM, Straube WL, Starman JD and Moros EG. Noninvasive temperature estimation based on the energy of backscattered ultrasound. Med Phys 2003; 30:1021-1029.

8. Seip R and Ebbini ES. Noninvasive estimation of tissues temperature response to heating fields using diagnostic ultrasound. IEEE Trans Biomed Eng 1995; 42:828-839.
9. Fallone BG, Moran PR and Podgorsak EB. Noninvasive thermometry with a clinical x-ray CT scanner. Med Phys 1982; 9:715-721.
10. Bentzen SM, Overgaard J and Jorgensen J. Isotherm mapping in hyperthermia using subtraction X-ray computed tomography. Radiother Oncol 1984; 2:255-260.
11. Zamenhof RG, Sternick ES and Curran BM. Coments on "Noninvasive thermometry with a clinical X-ray CT scanner". Med Phys 1983; 10:374.
12. Jenne JW, Bahner M, Spoo J, et al. CT on-line monitoring of HIFU therapy. IEEE Ultrasonics Symposium 1997; 1377-1380.
13. Dewey WC. Failla memorial lecture: The search for critical cellular targets damaged by heat. Radiat Res 1989; 120:191-204.
14. Lee RC and Astumian RD. The physicochemical basis for thermal and non-thermal 'burn' injuries. Burns 1996; 22:509-519.
15. Berland LL. Practical CT – Technology and techniques. Raven Press, New York 1987.
16. Yankelevitz DF, Henschke CI and Davis SD. Percutaneous CT biopsy of chest lesions: an in vitro analysis of the effect of partial volume averaging on needle positioning. AJR 1993; 161:273-278.
17. Welp C, Siebers S, Ermert H and Werner J. Investigation of the influence of blood flow rate on large vessel cooling in hepatic radiofrequency ablation. Biomed Tech (Berlin) 2006; 51:337-346.
18. Ritz J, Lehmann KS, Isbert C, et al. In-vivo evaluation of a novel bipolar radiofrequency device for interstitial thermotherapy of liver tumor during normal and interrupted hepatic perfusion. J Surg Res 2006; 133:174-184.
19. Rossi S, Garbagnati F, Francesco ID, et al. Relationship between the shape and size of radiofrequency induced thermal lesions and hepatic visualization. Tumori 1999; 85:128 – 132(abstract).

CHAPTER 4

Feasibility of noninvasive temperature assessment during radiofrequency liver ablation on computed tomography

J Comput Assist Tomogr 2011; 35:356 –360

G. D. Pandeya[1,3], M. J. W. Greuter[1], K. P. de Jong[2], B. Schmidt[3], T. Flohr[3], and M. Oudkerk[1]

1. *Department of Radiology, University Medical Center Groningen, University of Groningen, Groningen, The Netherlands;*
2. *Departments of Radiology and Hepato-Pancreato-Biliary Surgery and Liver Transplantation, University Medical Center Groningen, University of Groningen, Groningen, The Netherlands.*
3. *Siemens AG, Healthcare Sector, Forchheim, Germany;*

Abstract

Purpose:

The purpose of this study was to assess the feasibility of noninvasive thermometry using high-resolution computer tomography (CT) for the monitoring of bovine liver during radiofrequency (RF) ablation.

Methods:

Radiofrequency probes were used to ablate bovine livers from 20°C to 98°C. During the heating process, images were acquired using a multidetector CT scanner with simultaneous measurement of temperature using calibrated thermal sensors. The CT scanners thermal sensitivity was derived from the correlation between the CT numbers and temperature. The CT scanners thermal sensitivity was used to compute a temperature map, and this temperature map was overlaid on the original CT scan using a dedicated software application.

Results:

The CT numbers of the bovine liver showed a linear decline with an increase in temperature and a CT thermal sensitivity of -0.60 ± 0.026 Hounsfield unit/°C (R^2 = 0.87). Temperature maps were calculated using this correlation and were superimposed onto the CT scans presenting temperature distribution around the RF probe in the bovine liver.

Conclusions:

Noninvasive temperature determination is feasible during RF ablation of bovine liver using a high-resolution CT system. Therefore, the proposed method can be of potential use in clinical practice for noninvasive temperature mapping during ablation.

Introduction

Thermal ablation destroys malignant tumors by generation of heat. Several thermal ablation techniques, in combination with different imaging methods; have recently been described as minimally invasive strategies for the local treatment of malignant tumors [1-6]. All these ablation techniques are hampered by limited spatial and temporal information on the temperature distribution and, consequently, on thermal dose during the intervention procedure [1, 7]. A real-time map of the temperature distribution may help to achieve complete tumor ablation and spare vital structures. Thus, the real-time temperature map can improve the efficiency of thermal ablation and contribute to lessen the recurrence rate of tumors after ablation.

Temperature is the parameter governing tissue destruction in thermal ablation, and it induces cellular death via thermal coagulation. Therefore, the volume of ablation is indicated by the temperature distribution within the tissue. The spatial temperature distribution over the ablated region can be described by a bio-heat equation [8]. This equation describes that cytotoxicity is caused in the ablated tissue at temperatures higher than 50^{o}C for 4 to 6 minutes [9]. In addition, the ablated region heated higher than 55^{o}C becomes nonviable because of instantaneous cell death [10].

Radiofrequency (RF) ablation is the most widely used technique in clinical practice and is therefore used in this study. The required duration of RF ablation using thin metallic applicators is highly variable and depends on the type, size, and vascularization of the tumor [1, 11-13]. The spatial thermal distribution during RF ablation can be more irregular than expected, which may lead to

unpredictable thermal necrosis in and around the tumor [14, 15]. Thus, an incomplete ablation might occur, which is thought to be responsible for up to 60% of ablation site recurrences in, for instance, hepatic tumor treatment [16].

A real-time noninvasive assessment of the spatial temperature distribution during the ablation process is an attractive concept to visualize the 3-dimensional temperature distribution at the ablation zone and to improve the efficiency of the RF ablation. Ultrasound [17], magnetic resonance imaging [18, 19], and microwave radiometry [20] have been investigated for real-time imaging. In addition, few studies [21-23] have been done to investigate the use of computer tomography (CT). However, these CT studies have been performed using relatively low spatial and temporal resolution and only up to 55°C. Therefore, the aim of this study was to assess the feasibility of noninvasive temperature determination during the RF ablation of liver up to 98°C with current CT technology using submillimeter spatial resolution and subsecond temporal resolution.

Materials and methods

Theoretical Background

By definition, the mass attenuation coefficient (μ/ϱ) does not depend on the density (ϱ). Hence, the temperature dependence of the linear x-ray attenuation coefficient (μ) at temperature (T) can be written as,

$$\mu\,(T) = \left(\frac{\mu}{\rho}\right) \varrho(T). \qquad (1)$$

The definition of the CT number H is based on the linear attenuation coefficient of water (μ_w) at a reference temperature T_o,

$$H(T) = 1000\ \frac{\mu(T) - \mu_w(T_o)}{\mu_w(T_o)}. \qquad (2)$$

Now, from relation (1), (2) and the density-temperature relation ϱ = - (1/ α).δϱ/δT, in which α is the thermal expansion coefficient, it can be derived [24] that,

$$H(T) = \frac{H(T_o) + 1000}{1 + \alpha \Delta T} - 1000. \qquad (3)$$

This relation states that the CT number is dependent on temperature and on the thermal expansion coefficient.

In Vitro Sample Setup

Bovine liver retrieved from the animal was obtained from a local slaughter house and used for experiments within 12 hours of life termination of animal. Five cylindrical blocks of liver tissue with diameters of 90 mm and thicknesses of approximately 50 mm were prepared for 5 separate experiments. In each experiment, the liver tissue was placed into a plexi-glass cylinder with an internal diameter of 90 mm (Fig. 1). The liver tissue was heated using a multi-tined RF probe (LeVeen; Boston Scientific, Inc, Natick, Mass) in combination with an RF ablation system (Boston Scientific, Inc). The RF probe was inserted in the liver tissue from the central axis of the cylinder at a depth of approximately 40 mm. In addition, 5 calibrated thermocouple (NiCr-Ni) thermal sensors with a diameter of 0.25 mm were inserted through the end plate of the plexi-glass cylinder into the liver tissue up to a depth of approximately 53 mm and at a distance of approximately 2, 10, 15, 20, and 25 mm, respectively, from the RF probe (Fig. 1). The 5 thermal sensors were attached to a data logger (TopMessage; Delphine Technology, Bergisch Gladbach, Germany). The data logger was connected with a computer to store the temperature every second. During the

ablation, the liver tissue was heated from room temperature (20°C) up to 98°C as measured by thermal sensor 1 (Fig. 1).

Computed Tomographic Imaging

Each block of liver tissue was scanned with a SOMATOM Definition CT (Siemens AG, Forchheim, Germany) in single-source mode during the RF ablation procedure. In each procedure, 1 scan before ablation and at least 8 scans after ablation were performed with a time interval of approximately 3 minutes. All CT scans were acquired in sequential mode using 120 kV (peak), 200 mAs, a collimation of 12 x 1.2 mm, a field of view of 300 mm, and a temporal resolution of 250 milliseconds. The acquired images were reconstructed with a slice thickness of 1.2 mm, an increment of 1.2 mm, and a B31s kernel on a Syngo Acquisition Workplace (Siemens AG, Forchheim, Germany).

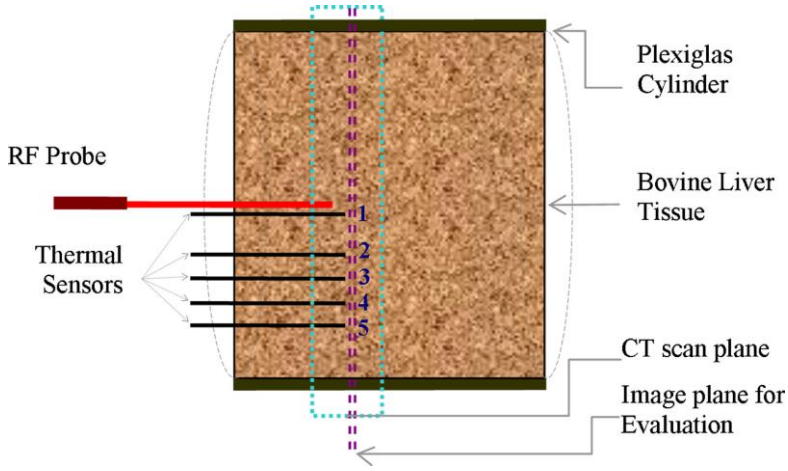

Figure 1
Schematic setup for bovine liver tissue inside a cylindrical plexiglass of internal diameter 90 mm. The RF probe was inserted from the central axis of the cylinder, and 5 thermal sensors were inserted at approximately 2, 10, 15, 20, and 25 mm from RF probe.

Data Analysis

The original CT data were loaded into a Syngo image viewer (Siemens AG, Forchheim, Germany) for the data analysis. In all 5 ablation procedures, all images that were directly adjacent to the images having the tip of the thermal sensors were chosen for evaluation. A circular region of interest (ROI) of approximately 100 mm was manually drawn in each selected image at the position of the 5 thermal sensors. The positions of thermal sensors are shown in Figure 3. From the ROI, the mean and SD of the CT numbers were measured. The SD observed in the measurements was used as an estimation of the CT noise. The measured mean values were correlated to temperature using a linear regression analysis. The goodness-of-fit was tested by calculating the correlation coefficient (R^2). Statistical analysis was performed using SPSS (v16.0.2; SPSS Inc, Chicago, Ill).

Temperature Mapping

The acquired image data were processed using a program developed under MevisLab environment (MevisLab 2.1; Mevis Medical Solutions AG, Bremen, Germany). Only CT scans acquired just at the end of the RF probe and close to the tip of the thermal sensors were used to avoid metal artifacts. First, all CT scans were masked using an upper and a lower CT number of 100 and -80 Hounsfield unit (HU), respectively, to exclude influences of the metallic thermal sensors and air or vapor pockets, respectively. Second, the images were smoothed using a 10 x 10 average convolution kernel (provided as in-built convolution kernel by MevisLab). The CT numbers at the selected region were converted into colors by using the correlation of the CT numbers and

temperature. The temperature maps were then overlaid on the original CT scans to show the temperature distribution near the RF probe.

Result

The mean CT number in the selected ROI was linearly dependent on temperature as shown in Figure 2. The noise within the selected ROI was approximately 6 HU. The CT thermal sensitivity was -0.60 ± 0.026 HU/^{o}C (R^2 = 0.87).

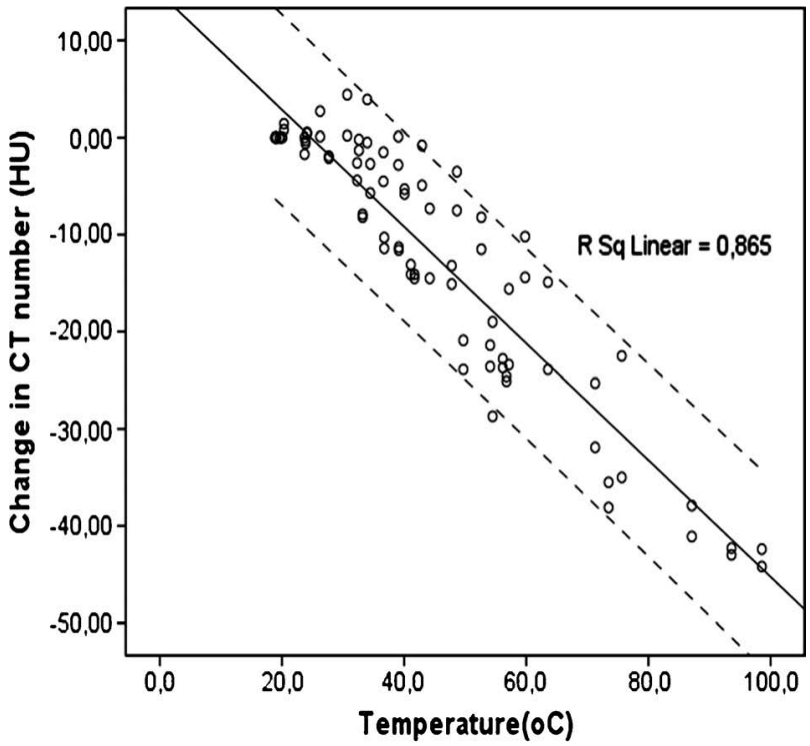

Figure 2

Changes in CT number as a function of temperature for bovine liver tissue. The central solid line represents a least-square linear fit. The stripped line represents the 95% prediction interval.

Computed tomographic scans during heating of the liver from 20°C to 98°C at the position of thermal sensor 1 (Fig. 1) are shown in Figure 3. The images showed a hypodense area near the RF probe, with a gradual decrease in CT numbers concomitant with a gradual increase in temperature from 20°C to 98°C. Furthermore, the hypodense area showed an increase in diameter as a function of time during RF ablation from Figure 3C to Figure 3I, whereas in Figures 3A and B, it is visibly not noticed. The correlation of CT number with temperature was translated into the color-coded temperature map shown in the lower part of Figure 3. The temperature map showed a relatively symmetric temperature distribution in liver tissue.

Figure 3 (see next page)
Example of CT scans (top) during RF ablation procedure in the bovine liver tissue. The central big circle indicates the position of multitined RF probe, and the other 5 small circles indicate the location of thermal sensors in adjacent image. The temperature measured by thermal sensor 1 was 20°C (A), 35°C (B), 53°C(C), 60°C(D), 71°C (E), 74°C (F), 87°C(G), 94°C(H), and 98°C (I). The corresponding temperature maps were overlaid in CT scans (bottom). The temperature was visualized according to the temperature bar as indicated.

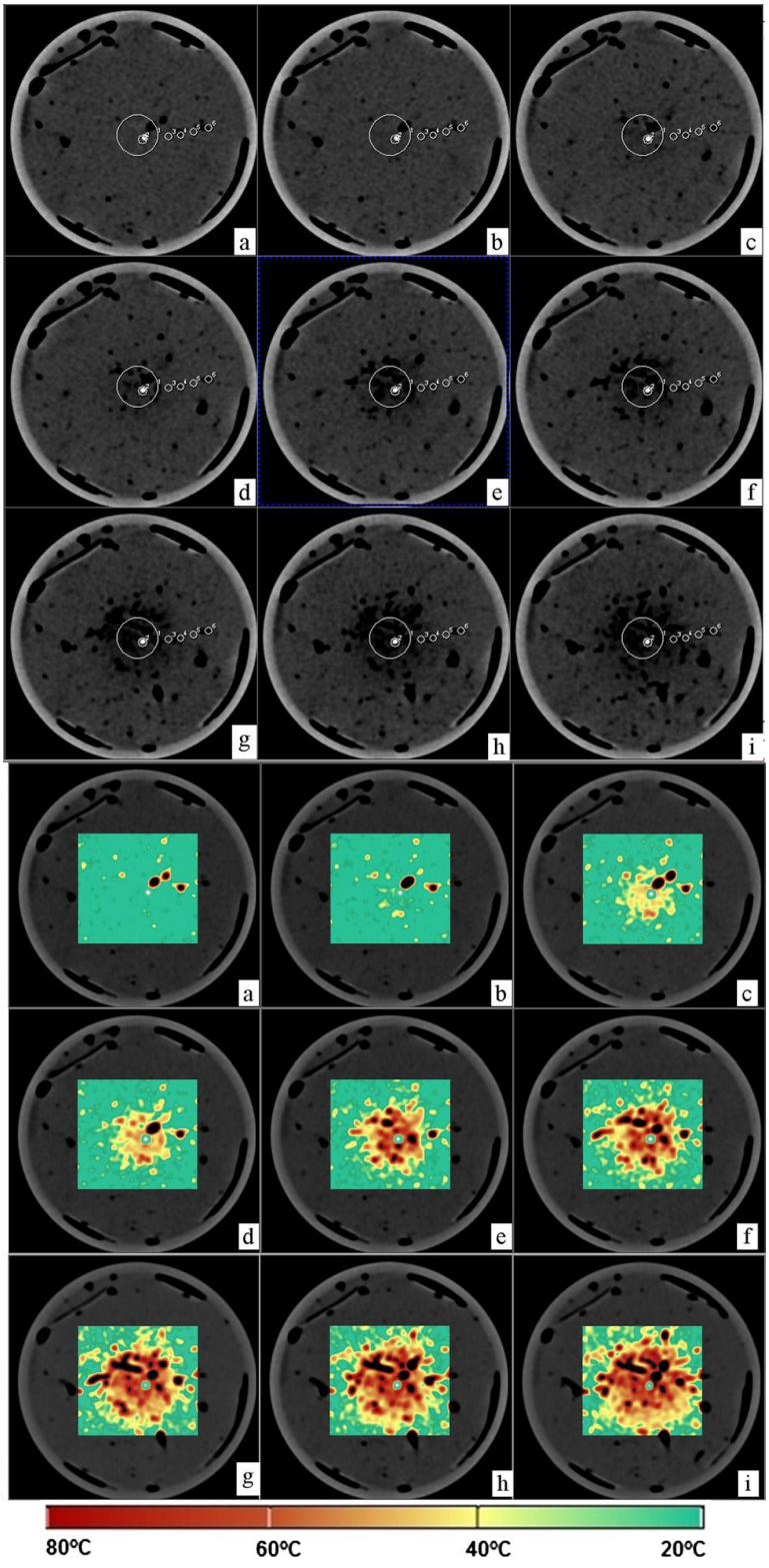
a
b
c
d
e
f
g
h
i
80°C
60°C
40°C
20°C

Discussion

This study shows that the CT number of liver is linearly dependent on temperature and that a CT thermal sensitivity of -0.60 HU/°C was obtained. The measured shifts in CT number were translated into a temperature map, which showed that a noninvasive assessment of temperature during ablation is feasible.

Fallone et al [21] reported a CT thermal sensitivity of -0.45 HU/°C for muscle tissue, whereas Jenne et al [23] reported -0.43 HU/°C for swine muscle tissue using high-intensity focus ultrasound. These results are in accordance with the present study, which also showed a linear dependency of CT number and temperature, but the quantitative results of the present study are more difficult to compare because they were obtained under different conditions of x-ray exposure, slice thickness, image acquisition time, and tissue materials.

Computed tomography parameters always play a major role in the evaluation of CT scans. Earlier studies [21, 23] were performed with relatively low spatial and temporal resolution, which may have reduced the accuracy of correlation of temperature measurement and CT numbers. During the ablation of tissues, the temperature drops very rapidly in a short distance from the ablation source. Therefore, a better spatial resolution and temperature resolution could provide a more accurate relation between CT numbers and measured temperature during 1 complete scan. Today's CT scanners offer subsecond scan times and submillimeter spatial resolution apart from other improved parameters. In this context, Bruners et al [25] estimated that the current CT scanner could realize a temperature resolution of 3 to 5°C. However, a desired

temperature resolution [7] of approximately 2°C could not be achieved in the present study because of the CT noise of 6 HU. Furthermore, the CT noise is expected to increase further in an in vivo examination because of the inhomogeneous structures and local physiological effects [22]. Therefore, further studies are needed to assess the feasibility of noninvasive temperature assessment with CT during RF ablation of the liver in a clinical setting.

The metal parts of the RF probe generated artifacts in the CT image and obscured absolute CT numbers in the proximity of the probe. However, the artifacts in the immediate vicinity of the RF probe are less cumbersome because temperature information is less demanding than at the border of the ablation area in the target volume. Therefore, the metal artifacts only influenced our results in the immediate vicinity of the RF probe. To obtain temperature information depending on CT numbers at the immediate vicinity of the RF probe, metal artifact reduction algorithms can be used. However, the CT numbers calculated by these metal artifact reduction algorithms are not reliable for quantitative evaluation yet [26] and hence cannot be used yet to obtain reliable temperature information.

Although the results in the present study were based on RF ablation of normal liver tissue, similar results are expected in tumor and other tissue types. The tissue damage occurs because of excessive physical forces between molecules when the temperature increases during ablation. The excessive physical forces can lead to various destructive cell processes such as rupturing of cell membrane, denaturation of proteins, and damage of ion channels [27, 28]. Hence, the tissue vulnerability to thermal damage depends on molecular structure and strength of chemical bonds but not on cell

size or shape [29]. Therefore, it is expected that the vulnerability to thermal damage is similar in different tissue types [27].

The color-coded temperature map showed in the present study can be used to derive the thermal dose, which is defined as the product of the temperature and the duration of the heat application. Furthermore, this map may be used to calculate the cumulative equivalent minute during low heating thermal therapy like hyperthermia [30]. Hence, a color-coded temperature map could improve the efficiency of thermal therapy by providing real-time temperature information of the ablation area.

Certain limitations of our ex vivo study should be considered when interpreting the results. First, the partial volume effect may give rise to unreliable CT numbers when the volume element represented by a pixel includes tissue components with highly different attenuation coefficients [31]. This effect is particularly important for the interpretation of CT numbers near the ablation electrode or near an air pocket at the ablation zone. Therefore, the acquired data were reconstructed in relatively thin slices (1.2 mm) to minimize the partial volume effect [32]. Next, the topology of the circular blocks of bovine liver tissue used in the present study did not represent an in vivo hepatic topology. In addition, the blocks of liver tissue were extracted from the side lobe of bovine liver excluding large blood vessels to ensure a near-homogeneous tissue structure. Next, the thermocouple might show a heat conduction effect on the temperature distribution in the present experimental setup. However, because very thin and mineral-insulated thermocouples (0.25 mm in diameter) were used at a relatively large distance from each other (5 mm), it is assumed that this effect does not significantly alter the results. Next, the tissue was not perfused, and

it is well known that vascular perfusion acts as a heat sink, which results in tissue cooling [33-35]. This effect needs to be evaluated during further experiments in perfused tissue samples. Next, some pixels near the gas pockets might be misregistered by the temperature color mapping process caused by a partial volume effect at the interface of tissue and gas pockets. However, we estimate that the influence of this effect on our results was minimal. Finally, the tissue received a relatively high radiation dose because of the repeated CT scans during the RF ablation. The radiation dose delivered in the present study was approximately 250 mGy per ablation experiment. This dose is well below the skin erythema threshold dose of 200 cGy. The total dose can be reduced by limiting the number of repeated CT scans. In addition, in the clinical setting, the total dose can be further reduced by optimizing the scan technique.

It has been shown that noninvasive temperature determination during RF ablation is feasible with current CT technology using submillimeter spatial resolution and subsecond temporal resolution. The real-time temperature map shows the spatial and temporal distribution of temperature during RF ablation. The method presented here could be used to assess noninvasive CT temperature mapping in an in vivo study.

Acknowledgments

The authors thank researchers and staff at the Department of Radiology, University Medical Center Groningen, in particular W.G.J. Tukker, Dr E.J.K. Noach, and Prof Dr E.J. van der Jagt. The authors also thank Peter Grininger and his team from Siemens AG, H IM CT for technical support.

References

1. Goldberg SN, Dupuy DE. Image-guided radiofrequency tumor ablation: challenges and opportunitiesVPart I. J Vasc Interv Radiol. 2001; 12:1021-1032.
2. Bischof JC, Mahr B, Choi JH, et al. Use of x-ray tomography to map crystalline and amorphous phases in frozen biomaterials. Ann Biomed Eng. 2007; 35:292-304.
3. Weld KJ, Landman J. Comparison of cryoablation, radiofrequency ablation and high-intensity focused ultrasound for treating small renal tumors. BJU Int. 2005; 96:1224-1229.
4. Cheng H-LM, Haider MA, Dill-Macky MJ, et al. MRI and contrast-enhanced ultrasound monitoring of prostate microwave focal thermal therapy: an in vivo canine study. J Magn Reson Imaging. 2008; 28:136-143.
5. Pacella CM, Bizzari G, Magnolfi F, et al. Laser thermal ablation in the treatment of small hepatocellular carcinoma: results in 74 patients. Radiology. 2001; 221:712-720.
6. Stauffer PR, Goldberg SN. Introduction: thermal ablation therapy. Int J Hyperthermia. 2004; 20:671-677.
7. Frich L. Non-invasive thermometry for monitoring hepatic radiofrequency ablation. Minim Invasive Ther Allied Technol. 2006; 1:18-25.
8. Pennes HH. Analysis of tissue and arterial blood temperature in the resting human forearm. J Appl Physiol. 1948; 1:93-122.
9. Goldberg SN, Gazelle GS, Halpern EF, et al. Radiofrequency tissue ablation: importance of local temperature along the electrode tip exposure in determining lesion shape and size. Acad Radiol. 1996; 3:212-218.
10. Nath S, Lynch C, Whayne G, et al. Cellular electrophysiological effects of hyperthermia on isolated guinea pig papillary muscle. Circulation. 1993; 88:1826-1831.
11. Brieger J, Pereira PL, Truebenback J, et al. In vivo efficiency of four commercial monopolar radiofrequency ablation systems, a comparative experimental study in pig liver. Invest Radiol. 2003; 38:609-616.
12. Denys A, Baere TD, Kuoch V, et al. Radiofrequency tissue ablation of the liver in vivo and ex vivo experiments with four different systems. Eur Radiol. 2003; 13:2346-2352.
13. Erdogan A, Grumbrecht S, Carlsson J, et al. Homogeneity and diameter of linear lesions induced with multipolar ablation catheter: in vitro and in vivo comparison of pulsed versus continuous radiofrequency energy delivery. J

Interv Card Electrophysiol. 2000; 4:655-661.
14. Pereira PL, Trubenbach J, Schenk M, et al. Radiofrequency ablation: in vivo comparison of four commercially available devices in pig livers. Radiology. 2004; 232:482-490.
15. Montgomery RS, Rahal A, Dodd GD, et al. Radiofrequency ablation of hepatic tumors: variability of lesion size using a single ablation device. AJR Am J Roentgenol. 2004; 182:657-661.
16. Mulier S, Ni Y, Jamart J, et al. Local recurrence after hepatic radiofrequency coagulation: multivariate meta-analysis and review of contributing factors. Ann Surg. 2005; 242:158-171.
17. Seip R, Ebbini ES. Noninvasive estimation of tissues temperature response to heating fields using diagnostic ultrasound. IEEE Trans Biomed Eng. 1995; 42:828-839.
18. Weidensteiner C, Quesson B, Caire-gana B, et al. Real time MR temperature mapping of rabbit liver in vivo during thermal ablation. Magn Reson Med. 2003; 50:322-330.
19. Lepetit-Coiffe M, Quesson B, Seror O, et al. Real time monitoring of radiofrequency ablation of rabbit liver by respiratory gated quantitative temperature MRI. J Magn Reson Imaging. 2006; 24:152-159.
20. Wang SS, VanderBrink BA, Regan J, et al. Microwave radiometric thermometry and its potential applicability to ablative therapy. J Interv Card Electrophysiol. 2000; 4:295-300.
21. Fallone BG, Moran PR, Podgorsak EB. Noninvasive thermometry with a clinical x-ray CT scanner. Med Phys. 1982; 9: 715-721.
22. Bydder GM, Kreel L. The temperature dependence of computed tomography attenuation values. J Comput Assist Tomogr. 1979; 3:506-510.
23. Jenne JW, Bahner M, Spoo J, et al. CT on-line monitoring of HIFU therapy. Proc IEEE Ultrasonics Symp. 1997; 2:1377-1380.
24. Homolka P, Gahleitner A, Nowotny R. Temperature dependence of HU values for various water equivalent phantom materials. Phys Med Biol. 2002; 47:2917-2923.
25. Bruners P, Levitt E, Penzkofer T, et al. Multi-slice computed tomography: a tool for non-invasive temperature measurement? Int J Hyperthermia. 2010; 26:359-365.
26. Barett JF, Keat N. Artifacts in CT: recognition and avoidance. Radiographics. 2004; 38:1679-1691.

27. Lee RC, Astumian RD. The physicochemical basis for thermal and non-thermal 'burn' injuries. Burns. 1996; 22:509-519.
28. Dewey WC. Failla memorial lecture. The search for critical cellular targets damaged by heat. Radiat Res. 1989; 120:191-204.
29. Breen MS, Breen MB, Butts K, et al. MRI-guided thermal ablation therapy: model and parameters estimates to predict cell death from MR thermometry images. Ann Biomed Eng. 2007; 35: 1391-1403.
30. Mertyna P, Dewhirst MW, Halpern E, et al. Radiofrequency ablation: the effect of distance and baseline temperature on thermal dose required for coagulation. Int J Hyperthermia. 2008; 24:550-559.
31. Berland LL. Practical CT: Technology and Techniques. New York, NY: Raven Press; 1987.
32. Yankelevitz DF, Henschke CI, Davis SD. Percutaneous CT biopsy of chest lesions: an in vitro analysis of the effect of partial volume averaging on needle positioning. AJR Am J Roentgenol. 1993; 161:273-278.
33. Welp C, Siebers S, Ermert H, et al. Investigation of the influence of blood flow rate on large vessel cooling in hepatic radiofrequency ablation. Biomed Tech (Berlin). 2006; 51:337-346.
34. Ritz J, Lehmann KS, Isbert C, et al. In-vivo evaluation of a novel bipolar radiofrequency device for interstitial thermotherapy of liver tumor during normal and interrupted hepatic perfusion. J Surg Res. 2006; 133:174-184.
35. Rossi S, Garbagnati F, De Francesco I, et al. Relationship between the shape and size of radiofrequency induced thermal lesions and hepatic visualization [abstract]. Tumori. 1999; 85:128-132.

CHAPTER 5

CT-based temperature monitoring during hepatic RF ablation: Feasibility in an animal model

Int J Hyperthermia 2012; 28:55–61

G. D. Pandeya[1*], P. Bruners[2,3*], E. Levit[3], E. Roesch[3], T. Penzkofer[2,3], P. Isfort[2,3], B. Schmidt[4], M. J.W. Greuter[1], M. Oudkerk[1], T. Schmitz-Rode[2], C. K. Kuhl[3], and A. H. Mahnken[3]

1. *Department of Radiology, UMC Groningen, University of Groningen, Groningen, The Netherlands*
2. *Applied Medical Engineering, Helmholtz Institutefor Biomedical Engineering, RWTH Aachen University, Aachen, Germany*
3. *Department of Diagnostic and Interventional Radiology, University Hospital, RWTH Aachen University, Aachen, Germany*
4. *Siemens Healthcare Sector, Forchheim, Germany*

* Both these authors contributed equally to the manuscript.

Abstract

Purpose: The aim of this paper was to establish non-invasive CT-based temperature monitoring during hepatic radio frequency (RF) ablation in an ex-vivo porcine model followed by transfer of the technique into a feasibility in-vivo experiment.

Materials and methods: Bipolar RF ablations were performed in 10 specimens of porcine liver. Parallel to the needle-shaped RF applicator three optical temperature probes were inserted into the liver specimens at fixed distances of 5, 10 and 15mm from the RF probe. During energy application (20W) unenhanced sequential MSCT scans were acquired using the following scan protocol: 140kV tube voltage, 300mAs/ rotation tube current time product, collimation 24x1.2mm, rotation time 0.5s. Axial image data was reconstructed using a soft tissue convolution kernel. Temperature data was recorded during every CT scan. Using a circular 0.5cm^2 regions of interest local CT values were measure at the tip soft he temperature probes and matched with the measured temperatures. Regression analysis was performed to analyze the relationship between local temperatures and CT values for each temperature probe position. Furthermore, the same experimental design was used in four anesthetized female pigs in order to investigate the potential of this technique for an in-vivo applicant.

Results: A negative correlation was found for the relationship between temperature and CT value. Regression coefficients were - 0.44 (5mm), - 0.35 (10mm) and - 0.37 (15mm) for ex-vivo data. Analysis is of in-vivo experiments showed regression coefficients between - 0.025 and - 0.434.

Conclusion: Multi slice computed tomography is able to depict temperature changes in liver tissue during RFA.

Introduction

Hyperthermal ablation therapies offer a potentially curative treatment option for patients who are not candidates for surgical section due to severe comorbidities. Besides microwave ablation(MWA) [1,2], high intensity focused ultrasound(HIFU) [3] and laser induced thermometry(LITT) [4], radio-frequency(RF) ablation found its way into clinical routine during the last decade as a minimally invasive therapy for different malignancies of lung[5], kidneys[6] and bone[7]. However, most often RF ablation is used for treating primary or secondary malignant hepatic tumours [8–11]. In applying hepatic RF ablation with curative intent, complete tumour coagulation including a safety margin of at least 0.5–1.0 cm is crucial. In order to achieve nearly instantaneous protein denaturation a local temperature of 60°C must be achieved [12]. Non-invasive thermometry during RF energy application would allow assessing the temperature distribution within the target volume and thereby help the interventionalist to decide whether complete tumour ablation is achieved. Furthermore, collateral thermal damage of structures located near the ablation volume could be avoided. So far, magnetic resonance imaging (MRI)-based thermometry, ultrasound thermometry, microwave-based thermometry and electrical impedance tomography were shown to have the potential of measuring temperature non-invasively [13]. Lately, the temperature-dependent shift of CT numbers, which has been known for more than thirty years, was investigated in an in vitro study using a modern clinical CT scanner [14]. The reported temperature dependency of the measured CT values may provide the base for a non-invasive temperature measurement during hyperthermal ablation therapies.

Therefore, the aim of our study was to investigate whether multi-slice CT is able to depict local temperature changes during hepatic RF-ablation in an ex-vivo and an in-vivo setting.

Materials and method

Ex-vivo experiments

Freshly excised porcine livers, which were obtained from the Institute for Veterinary Medicine, were cut into ten pieces of approximately 10x5x4 cm. A single specimen was placed on a paper plate and the bipolar RF-applicator (Celon ProSurge T30, Celon AG, Teltow, Germany) was inserted at a depth of at least 3.5 cm. In order to measure spatial temperature changes during the RF ablation, three optical temperature probes (SFF-2 m, Luxtron Corporation, Santa Clara, CA, accuracy ±2°C) were additionally inserted into the liver specimen with their tips being located 5, 10

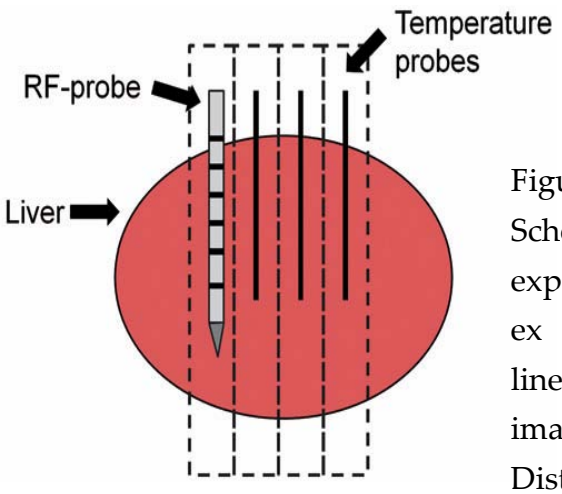

Figure 1
Schematic drawing of the experimental setup used for the ex vivo study. The scattered lines represent the axial CT images that were reconstructed. Distances between RF applicator and temperature probes were 5, 10 and 15 mm, respectively.

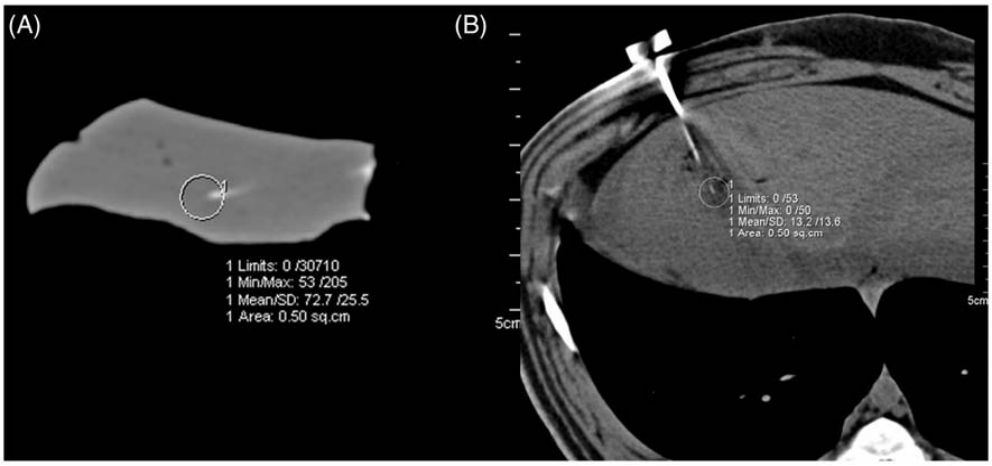

Figure 2

Examples for ex vivo (A) and in vivo (B) measurements of local temperature around the tip of a temperature probe during Radiofrequency ablation. Note the beam hardening artifacts in (B) caused by the RF-applicator.

and 15 mm away from the middle of the active tip of the RF probe (Figure 1). Thereafter, the prepared liver block was placed in the isocenter of a 64-slice dual source CT scanner (SOMATOM Definition, Siemens, Forchheim, Germany), with the RF applicator and the temperature sensors being placed perpendicular to the scanner's z-axis. During the RF ablation, which was performed with a generator output of 20 W as recommended by the vendor, sequential CT examinations without table movement (28.8 mm z-coverage) were performed every 15 s employing the following scan protocol: 120 kV tube voltage, 320 mAs/rotation tube current time product, 24x1.2 mm collimation, 0.5 s rotation time. Prior to each scan series the implemented check-up procedure including a scanner calibration in air was performed. After raw data acquisition a soft tissue convolution kernel (B40s) and a 512x512 matrix were

used for reconstruction of axial images with a slice thickness of 2.4 mm. A slice thickness of 2.4 mm was chosen in order to reduce image noise. For image data analysis local CT numbers were measured using a circular 0.5 cm^2 region of interest (ROI) that was placed centrally around the tip of each temperature probe at each image data acquisition time-point as shown in Figure 2. The measured CT numbers were matched with the temperature measured at the same time. In total, 10 ex-vivo experiments as described above were performed.

In-vivo experiments

After approval from the official committee on animal affairs four female pigs with a weight of 70 kg were included in this study. After intramuscular premedication with a combination of atropine (Atropinum sulphuricum solution 1%, WDT, Garbsen, Germany), azaperone (Stresnil, Janssen-Cilag, Neuss, Germany) and ketamine (Ketamin 10%, Ceva Tiergesundheit, Du¨sseldorf, Germany) anesthesia was induced using diluted pentobarbital (Narcoren, Merial, Hallbergmoos, Germany), which was injected using a 18 gauge venous access placed in an ear vein. The animals were intubated and mechanically ventilated (Sulla 808, Draeger Medical, Luebeck, Germany) with an oxygen–air mixture containing 1.0 vol% Isoflurane to maintain anesthesia. For additional analgesia animals received a fentanyl drip via the venous access line and 1 L of 0.9% saline infusion in order to prevent dehydration.

All in-vivo experiments were performed using the same CT system (SOMATOM) as for the previous ex-vivo study. Animals were placed on the CT table in supine position and moved to the isocentre of the CT gantry. After acquisition of a non-enhanced

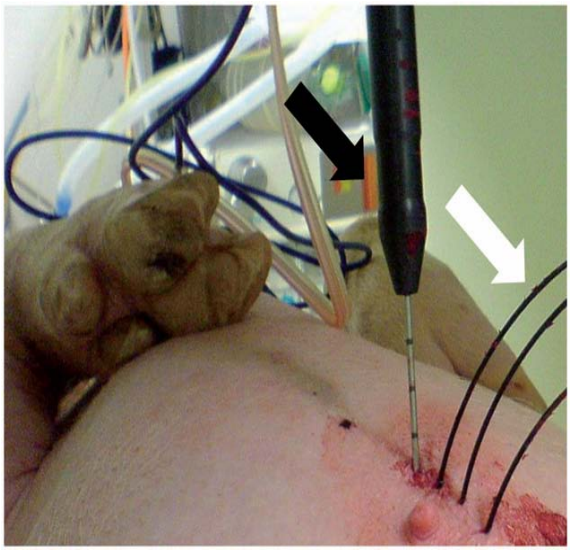

Figure 3
Experimental setup used for the in-vivo experiments with the animal lying in supine position. RF applicator (black arrow) and three temperature probes (white arrow) are inserted parallel.

spiral CT scan in end-expiratory breath hold (64x0.6 mm collimation, 120 kV tube voltage, 165 mAs/rotation tube current time product, 0.5 s gantry rotation time), RF probe placement via an anterior strictly in-plane approach was planned using the implemented CT scanner software. After cleaning of the skin the RF applicator was advanced along the planned puncture path under repetitive sequential unenhanced CT scans. Then three optical temperature probes were additionally inserted parallel to the RF probe with a fixed distance of 5, 10 and 15 mm to the middle of the active tip (Figure 3) using positioning device. In our experiments RF applicator and temperature probes were inserted mostly in the same part of the liver in all cases. After the start of the RF ablation, sequential CT scans were performed using 140 kV tube voltage and 300 mAs/rotation tube current time product, a collimation of 24x1.2 mm, and a rotation time of 0.5 s. Axial image data was reconstructed at a slice thickness of 1.2 mm using a B31 smooth kernel. During performance of CT scans temperature data were read out from the thermal sensors continuously throughout the RF

ablation using a serial port and a custom-made software tool. As described above for the ex-vivo study area, averaged CT numbers were measured at the tip of the temperature probes at every image data acquisition time-point using a 0.5 cm^2 ROI as shown in Figure 2 and matched to the corresponding temperature data.

RF ablation system

All RF-ablations were performed with a bipolar RF system (CelonLabPower, Celon Medical Instruments, Teltow, Germany) which operates at a frequency of 470 kHz and provides a variable power output between 2 and 250 W. The used RF applicator features an active tip of 30 mm (Celon ProSurge T30) and an internal cooling with 0.9% saline solution delivered by a peristaltic pump at a flow rate of 30 mL/min. As recommended by the manufacturer the generator output was set to 20 W. The RF system was operated at the ''resistance controlled automatic power mode'', which means that the power output automatically adjusted to the measured tissue impedance in order to avoid early tissue dehydration. During RF ablations the applied power, tissue resistance, and application time were monitored using a dedicated software tool (CelonPowerMonitor Version 2.6).

Statistical analysis

For ex-vivo experiments a linear regression analysis was performed to analyse the relationship between temperature and measured CT values. Therefore, temperature data from the 10 ex-vivo experiments was pooled for each temperature probe position (5, 10, 15 mm distance to the RF-applicator) and matched to the corresponding CT numbers.

For in-vivo experiments a linear regression analysis was performed for each thermal sensor position in every animal. A p value <0.05 was considered statistically significant. All analyses were performed using SAS Software 9.1.3 (SAS Institute, Cary, NC).

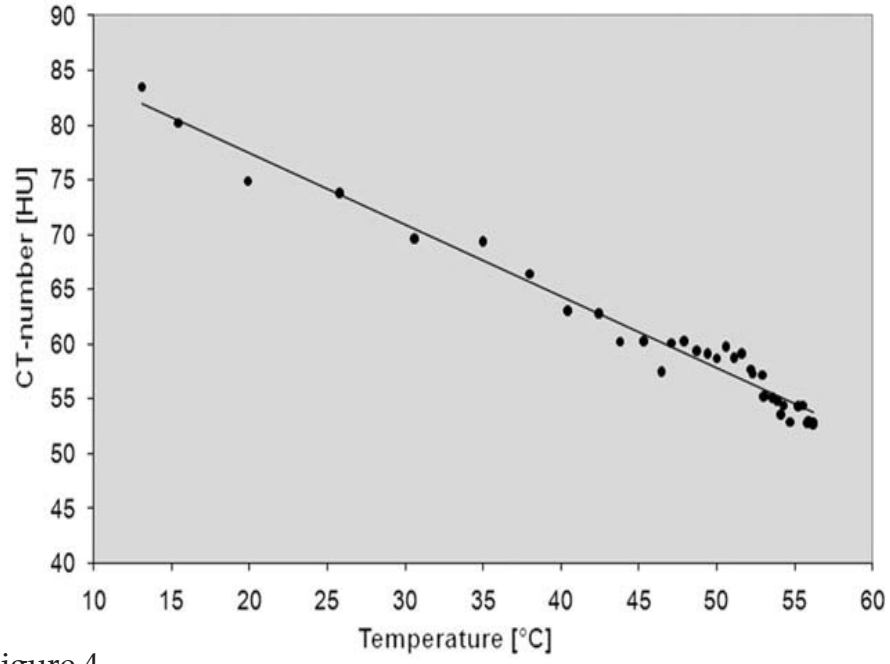

Figure 4
The scatter diagram for a single ex-vivo experiment.

Table I. Results of the ex-vivo study. Temperature data and measured CT-numbers derived from the 10 experiments were pooled for each temperature probe position.

Distance to RF-probe	Number of measurements (n)	Intercept	Regression Coefficient
5 mm	379	77.02	-0.44
10 mm	371	74.42	-0.35
15 mm	373	79.57	-0.37

Table II. Results of the in-vivo study

In-vivo experiment #	Distance to RF-probe	Number of measurements (n)	Intercept	Regression Coefficient
1	5 mm	30	27.59	-0.03
	10 mm	28	39.79	-0.18
	15 mm	30	43.46	-0.32
2	5 mm	42	22.12	-0.43
	10 mm	43	49.12	-0.30
	15 mm	43	37.09	-0.13
3	5 mm	43	28.99	-0.03
	10 mm	43	50.72	-0.31
	15 mm	43	38.97	-0.16
4	5 mm	41	42.29	-0.16
	10 mm	41	48.36	-0.23
	15 mm	41	55.17	-0.30

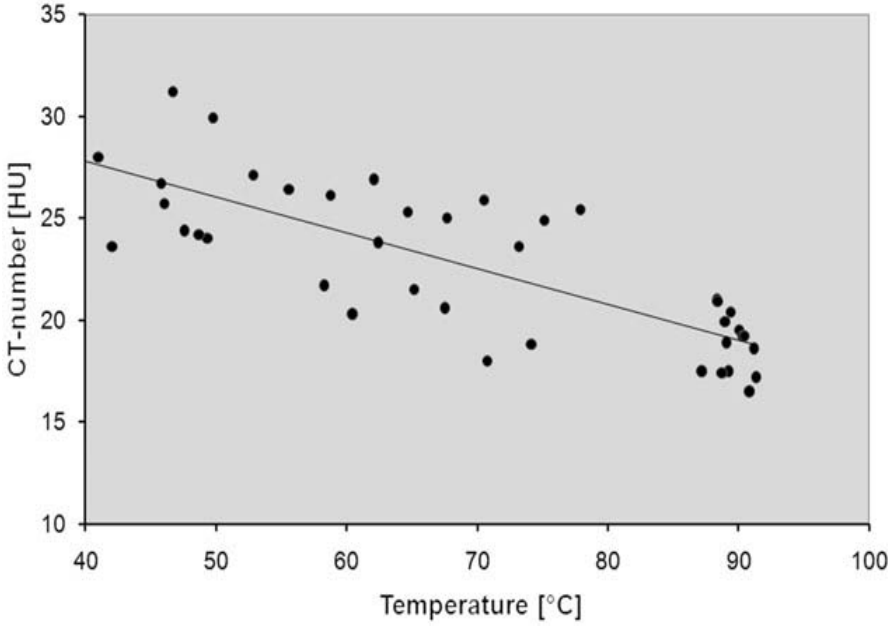

Figure 5
The scatter diagram for a single in-vivo experiment.

Results

Ex-vivo study

The regression analysis showed a negative relationship between measured temperature during RF-ablations and the area-averaged CT numbers. Results are summarised in Table I. Regression coefficients varied between -0.44 (5 mm distance to the RF applicator) and -0.35 (10 mm distance to the RF applicator) as shown in Figure 4.

In-vivo study

The results of the in-vivo study also show negative regression coefficients for the relationship between temperature and CT

numbers for all temperature probes in every animal ranging from -0.025 (p value: 0.1721) to -0.432 (p value: 0.0050) as shown in Figure 5. The CT value measurements at the tip of the temperature probe being located 5 mm away from the RF-probe were especially hampered by metal artifacts caused by the RF applicator in the in-vivo experiments. Results are summarised in Tables II.

Discussion

As recently published by Frich [13], the ideal requirements for non-invasive temperature measurements during hyperthermal ablation therapies include a temperature accuracy of 1–2°C, a spatial resolution of <1–2 mm and an acquisition time of <10–30 s. Furthermore, the three dimensional temperature distributions should be presented in real time to allow for correction of RF applicator placement or adjustment of the RF energy delivery. In addition, the ideal non-invasive thermometry should be insensitive to motion of the patient and be compatible with commonly used ablation devices as well as with the used imaging modality.

So far, mainly MRI and ultrasound have been used for non-invasive temperature mapping during hyperthermal ablation therapies in the liver. Non-invasive MR thermometry is based on the temperature dependency of different MR parameters. Initially, the temperature-dependent change of longitudinal relaxation time was used for noninvasive temperature mapping [15]. Other MR parameters which provide a potential base for noninvasive thermometry are the proton resonance frequency of tissue water, the diffusion coefficient, and the proton density [16]. Also, temperature-sensitive contrast agents can be used for quantification of local temperature [17]. In contrast to RF ablation, which suffers

from the usage of metallic applicators and interferences between the RF generator and the MR scanner, LITT is a suitable hyperthermal ablation technique to be monitored with MR thermometry. But different technical solutions have also been explored for MR-guided RF-ablation to overcome the limitations mentioned, such as interleaving of RF ablation cycles and MR data acquisition [18], filtering [19, 20] and the use of MR-compatible RF-applicators [21]. Several ultrasonic parameters provide a basis for non-invasive thermometry as well. These parameters include the temperature-dependent echo shifts due to changes in tissue thermal expansion and speed of sound, the attenuation coefficient and change in backscattered energy due to tissue in homogeneities [22]. Other, more experimental techniques for non-invasive temperature measurements which could potentially be used during hyperthermal ablation procedures include microwave computed tomography and electrical impedance tomography.

A non-invasive thermometry during RF ablation based on the temperature dependency of CT numbers would be beneficial due to several reasons:

(1) There is no need for special RF equipment because all commercially available RF systems are compatible with modern CT scanners and only one single case-report refers to a potential electromagnetic cross-talk between a CT system and an operating RF generator during hepatic RF ablation resulting in severe imaging artifacts [25].

(2) CT guidance for the placement of RF applicators is widely used due to broad availability of CT scanners providing a high spatial resolution, an acceptable soft tissue contrast and the possibility to detect immediate complications like bleeding.

(3) The additional option to perform a CT-based thermometry during RF ablation would allow improvement of the safety of the procedure by depiction of temperature around vital structures being located in the vicinity of the target volume. The three-dimensional visualisation of temperature distribution would also be helpful to decide whether the induced coagulation volume completely covers the target lesion including a safety margin of at least 0.5 cm and thereby reduces the risk for incomplete ablation.

First data concerning the temperature dependency of CT attenuation values in water and biological tissue was published in the late 1970s [23]. Fallone et al. published in vitro data about the decrease of CT numbers during the heating of water and muscle tissue [24]. They postulated an achievable temperature discrimination of less than 1°C at a spatial resolution of the order of 1 cm based on CT value thermal shift of 0.4 and 0.45 HU/°C for water and muscle tissue, respectively. But due to technical CT scanner limitations this approach was not further investigated. The results of the presented ex-vivo experiments using state-of-the-art CT technology show a temperature-dependent shift of CT values between -0.35 and -0.44 HU/°C. However, the transfer into the in-vivo study showed some major problems as reflected by the regression coefficient (-0.03) which was calculated for the temperature probe at 5 mm distance from the RF probe in pig 1 (Table II) and pig 3 (Table IV). Metal artifacts and beam hardening (Figure 2) as well as vaporisation hamper a reliable measurement of local CT-numbers in the direct vicinity of the RF probe especially.

In contrast to the ex-vivo study, the image data of the in-vivo experiments show the severe beam hardening artifacts which distort the measurement of CT numbers. This observation is due to

the fact that in ex-vivo experiments the RF probe could be placed exactly in the scan plane. That is why significant beam hardening artifacts only occur in the slice showing the RF probe, and much less in the slices depicting the temperature probes. In contrast, in the in-vivo experiments a strictly in-plane placement of the RF probe in the living animal was hard to achieve, which led to more severe beam-hardening artifacts. Newly developed algorithms for metal artifact reduction may help to overcome this issue [26]. Furthermore, as reflected by Figures 4 and 5 the scatter of CT numbers is clearly larger in the in-vivo experiments when compared to the ex-vivo situation. A reason for this observation may be that the ex-vivo liver specimens provide a quite homogenous subject with a uniform heat distribution. In contrast, in the in-vivo experiments blood flow leads to the typical heat-sink effect around vessels, resulting in irregular heat propagation. Although we tried to avoid placement of temperature probes in the vicinity of large vessels, it sometimes occurred, as only unenhanced CT scans were used for RF applicator and thermal sensor positioning. With regard to the measurements at the outer rim of the ablation zone, the induced local hyperaemia, which surrounds the ablation volume, may also contribute to inhomogeneous local temperature distribution and thereby hamper a reliable CT-based thermometry. This aspect may be the reason for the lowest regression coefficient being seen at the largest distance from the RF probe in pig 2 (Table III).

Using multi-slice CT as the base for in-invasive thermometry in a clinical context will require an individual calibration process because of the significant inter-and intra-scanner variability of CT numbers [27]. Moreover, the individual composition of liver tissue, e.g. in patients suffering from liver cirrhosis or hepatic steatosis,

will influence the temperature dependency of CT numbers. Therefore, the use of a RF applicator featuring an integrated thermocouple being located at a certain distance from the active tip can be a useful tool for an individual patient calibration process. Alternatively the insertion of a separate optical temperature probe into the target volume could be used for this purpose.

A visualisation of temperature-dependent changes of CT numbers during RFA may be realised as a colour-coded image based on image subtraction [28, 29] that is superimposed on a pre-interventionally acquired diagnostic examination showing the target lesion. If a reliable registration of both scans can be assumed this would allow the evaluation of the local temperature distribution within the target volume. Local bleeding within the target volume due to RF applicator placement may lead to an increase of local CT numbers and thereby can inhibit a detection of temperature changes. Also the intravenous administration of contrast agent immediately before or during the RF ablation would hinder a CT-based temperature monitoring.

The study presented suffers from some limitations that need to be discussed. First, the study population includes only four animals which are only suited to show the feasibility of MSCT to depict temperature-dependent changes of hepatic tissue. Hence, further in-vivo and clinical studies are needed to confirm the presented results. Furthermore, the temperature dependency of CT numbers was investigated in healthy porcine liver parenchyma which may differ from pathologically altered human liver tissue. This limits the transfer of the results into the clinical situation. Also, the manual measurement of CT numbers using a small circular ROI needs to be improved by a more accurate and robust software-based method

which might also improve the achievable spatial resolution.

In conclusion, the presented data shows an inverse relationship between local temperature and area-averaged CT numbers during hepatic RF ablation in ex-vivo and in-vivo porcine models. This finding may provide the basic principle for CT-based non-invasive thermometry during hyperthermal ablation procedures.

Declaration of interest: The authors report no conflicts of interest. The authors alone are responsible for the content and writing of the paper. Bernhardt Schmidt is an employee of Siemens Healthcare.

References

1. Bhardwaj N, Strickland AD, Ahmad F, et al. Microwave ablation for unresectable hepatic tumours: Clinical results using a novel microwave probe and generator. Eur J Surg Oncol 2010; 36:264–268.
2. Ryan TP, Turner PF, Hamilton B. Interstitial microwave transition from hyperthermia to ablation: Historical perspectives and current trends in thermal therapy. Int J Hyperthermia 2010; 26:415–433.
3. Park MY, Jung SE, Cho SH, et al. Preliminary experience using high intensity focused ultrasound for treating liver metastasis from colon and stomach cancer. Int J Hyperthermia 2009; 25:180–188.
4. Vogl TJ, Straub R, Eichler K, et al. Colorectal carcinoma metastases in liver: Laser-induced interstitial thermotherapy—local tumor control rate and survival data. Radiology 2004; 230:450–458.
5. De Baere T, Palussiere J, Auperin A, et al. Midterm local efficacy and survival after radiofrequency ablation of lung tumors with minimum follow-up of 1 year: Prospective evaluation. Radiology 2006; 240:587–596.
6. Tracy CR, Raman JD, Donnally C, et al. Durable oncologic outcomes after radiofrequency ablation: Experience from treating 243 small renal masses over 7.5 years. Cancer 2010; 116:3135–3142.
7. Dupuy DE, Liu D, Hartfeil D, et al. Percutaneous radiofrequency ablation of painful osseous metastases: A multicenter American College of Radiology Imaging Network trial. Cancer 2010; 116:989–997.

8. Pereira PL. Actual role of radiofrequency ablation of liver metastases. Eur Radiol 2007; 17:2062–2070.
9. Lencioni R, Cioni D, Crocetti L, et al. Early-stage hepatocellular carcinoma in patients with cirrhosis: Long-term results of percutaneous image-guided radiofrequency ablation. Radiology 2005; 234:961–967.
10. Mulier S, Ruers T, Jamart J, et al. Radiofrequency ablation versus resection for resectable colorectal liver metastases: Time for a randomized trial? An update. Dig Surg 2008; 25:445–460.
11. Kim HR, Cheon HS, Lee KH, et al. Efficacy and feasibility of radiofrequency ablation for liver metastases from gastric adenocarcinoma. Int J Hyperthermia 2010; 26:305–315.
12. Goldberg SN, Dupuy DE. Image-guided radiofrequency tumor ablation: Challenges and opportunities—Part I. J Vasc Interv Radiol 2001; 12:1021–1032.
13. Frich L. Non-invasive thermometry for monitoring hepatic radiofrequency ablation. Minim Invasive Ther Allied Technol 2006; 15:18–25.
14. Bruners P, Levit E, Penzkofer T, et al. Multi-slice computed tomography: A tool for non-invasive temperature measurement? Int J Hyperthermia 2010; 26:359–365.
15. Parker DL, Smith V, Sheldon P, et al. Temperature distribution measurements in two-dimensional NMR imaging. Med Phys 1983; 10:321–325.
16. Rieke V, Butts Pauly K. MR thermometry. J Magn Reson Imaging 2008; 27:376–390.
17. Quesson B, de Zwart JA, Moonen CT. Magnetic resonance temperature imaging for guidance of thermotherapy. J Magn Reson Imaging 2000; 12:525–533.
18. Botnar RM, Steiner P, Dubno B, et al. Temperature quantification using the proton frequency shift technique: In vitro and in-vivo validation in an open 0.5 Tesla interventional MR scanner during RF ablation. J Magn Reson Imaging 2001; 13:437–444.
19. Gellermann J, Faehling H, Mielec M, et al. Image artifacts during MRT hybrid hyperthermia – Causes and elimination. Int J Hyperthermia 2008; 24:327–335.
20. Mertyna P, Dewhirst MW, Halpern E, et al. Radiofrequency ablation: The effect of distance and baseline temperature on thermal dose required for coagulation. Int J Hyperthermia 2008; 24:550–559.

21. Mahnken AH, Buecker A, Spuentrup E, et al. MR-guided radiofrequency ablation of hepatic malignancies at 1.5 T: Initial results. J Magn Reson Imaging 2004; 19:342–348.
22. Arthur RM, Straube WL, Trobaugh JW, Moros EG. Noninvasive estimation of hyperthermia temperatures with ultrasound. Int J Hyperthermia 2005; 21:589–600.
23. Bydder GM, Kreel L. The temperature dependence of computed tomography attenuation values. J Comput Assist Tomogr 1979; 3:506–510.
24. Fallone BG, Moran PR, Podgorsak EB. Noninvasive thermometry with a clinical X-ray scanner. Med Phys 1982; 9:715–721.
25. Brennan DD, Appelbaum L, Raptopolous V, et al. CT artifact introduced by radiofrequency ablation. Am J Roentgenol 2006; 186:S284–286.
26. Mahnken AH, Raupach R, Wildberger JE, et al. A new algorithm for metal artifact reduction in computed tomography: In vitro and in-vivo evaluation after total hip replacement. Invest Radiol 2003; 38:769–775.
27. Birnbaum BA, Hindman N, Lee J, Babb JS. Multi-detector row CT attenuation measurements: Assessment of intra-and interscanner variability with an anthropomorphic body CT phantom. Radiology 2007; 242:109–119.
28. Bentzen SM, Overgaard J, Jorgensen J. Isotherm mapping in hyperthermia using subtraction X-ray computed tomography. Radiother Oncol 1984; 2:255–260.
29. Minhaj AM, Mann F, Milne PJ, et al. Laser interstitial thermotherapy (LITT) monitoring using high-resolution digital mammography: Theory and experimental studies. Phys Med Biol 2002; 47:2987–2999.

CHAPTER 6

Feasibility of computed tomography based thermometry during interstitial laser heating in bovine liver

Eur Radiol 2011; 21:1733–1738

G. D. Pandeya[1,3], J. H. G. M. Klaessens[2], M. J. W. Greuter[1], B. Schmidt[3], T. Flohr[3], R. van Hillegersberg[4] and M. Oudkerk[1]

1. Department of Radiology, UMC Groningen, University of Groningen, The Netherlands
2. Department of Medical technology and Clinical Physics, UMC Utrecht, Utrecht, The Netherlands
3. H IM CT PLM-E PA, Siemens AG, Forchheim, Germany
4. Department of Surgical Oncology, UMC Utrecht, Utrecht, The Netherlands

Abstract

Objectives

To assess the feasibility of computed tomography (CT) based thermometry during interstitial laser heating in the bovine liver.

Methods

Four freshly exercised cylindrical blocks of bovine tissue were heated using a continuous laser of Nd:YAG (wavelength: 1064 nm, active length: 30mm, power: 10-30W). All tissues were imaged at least once before and 7 times during laser heating using CT and temperatures were simultaneously measured with 5 calibrated thermal sensors. The dependency of the average CT numbers as a function of temperature was analysed with regression analysis and a CT thermal sensitivity was derived.

Results

During laser heating, the growing hypodense area was observed around the laser source and that area showed an increase as a function of time. The formation of hypodense area was caused by declining in CT numbers at increasing temperatures. The regression analysis showed an inverse linear dependency between temperature and average CT number with -0.65 ±0.048 HU/^{o}C (R^2 = 0.75) for the range of 18 – 85^{o}C in bovine liver.

Conclusions

The non-invasive CT based thermometry during interstitial laser heating is feasible in the bovine liver. CT based thermometry could be further developed and may be of potential use during clinical LITT of the liver.

Introduction

Thermal ablative techniques such as laser, radiofrequency (RF), and microwave have gained interest as effective and safe alternatives for many patients [1, 2, 3]. However, laser-induced interstitial thermotherapy (LITT) is capable of destroying not only liver metastases with an improved survival rate, but also other abdominal tumours [4, 5]. Despite minor complications such as hepatic abscesses, bile duct injury and liver segmental infarction, low complication rates (< 2%) were reported for LITT [6, 7]. The complete tumour ablation is usually hampered by limited temperature information during LITT. Thus, a method to extract temperature information is required and especially, method needs to be non-invasive approach. Such method may improve the efficiency of LITT.

Laser-induced interstitial thermotherapy is mostly performed via interstitial fibres with 10- to 40-mm cylindrical diffusing tips [8], using a Nd:YAG (Neodymium:Yttrium-Aluminium-Garnet) laser at 1064 nm because of its optimal penetration at the near-infrared range of the spectrum [9]. The laser heating by direct penetration is increased in malignant tissue than normal tissue because of a decrease in anisotropy, absorption and scattering coefficients. Temperatures above 60^{o}C will cause rapid coagulative necrosis, temperatures above 100^{o}C will cause vaporisation [9], and temperatures above 300^{o}C will cause carbonisation. This carbonisation reduces optical penetration and heat conduction and, therefore, limits the size of the ablation area. The use of saline-cooled sheaths prevents carbonisation and allows for higher laser powers up to 50 W compared with 5 W without cooling sheaths [10].

During LITT, non-invasive temperature monitoring is required to achieve complete tumour necrosis without damaging critical anatomical structures [11]. Moreover, this process is essential to avoid local recurrence. Recently, various techniques such as ultrasound imaging [12], MR imaging [13, 14] and microwave radiometry [15] have been under investigation for non-invasive thermometry. Among these imaging techniques, MR thermal imaging has shown a temperature accuracy of ± 1°C. However, MR has relatively long acquisition times and is therefore sensitive to motion and misregistration artefacts [16, 17]. Although few studies [18, 19] reported the temperature dependency using modern Computed Tomography (CT) but CT has not been explored to monitor temperatures during LITT in clinical practice.

Therefore, the aim of the present study is to assess the feasibility of non-invasive CT based thermometry during laser heating of liver tissue in an ex-vivo setting.

Materials and methods:

The study was conducted after obtaining approval from the institutional ethical committee for animal care. Bovine livers were extracted from animals and four cylindrical blocks of liver tissue with 90 mm in diameter and approximately 50 mm in thickness were dissected within 12 hours of sacrifice. Each circular block of liver tissue was placed into a Perspex cylinder of 90 mm in internal diameter (Fig. 1).

Laser heating was performed with an Nd:YAG laser (TT Yag-80; Trumpf Medizine Systeme, Umkirch, Germany) at a wavelength of 1064 nm. The laser light was delivered through a quartz fibre with a core diameter of 400µm and was diffused using an applicator with

a length of 30 mm (Microflexx 30, KLS Martin GmbH, Umkirch, Germany). The fibre was placed into a cooling sheath (Lightcath, Trumpf Medizine Systeme, Umkirch, Germany). The cooling sheath with the laser fibre was inserted through the central hole (diameter: 5 mm) in the top of the Perspex cylinder into the liver tissue at a depth of 50 mm. Each of the four liver tissue blocks were heated using laser with a power from approximately 10 to 30 W in 5W interval. Laser heating was put off when temperature measured by thermal sensor 1 was reached 85^{o}C in each experiment.

Five calibrated thermocouple (NiCr-Ni) thermal sensors of 0.25 mm in diameter were inserted through holes (1 mm in diameter) in the top of the Perspex cylinder at 10, 15, 20, 25 and 30 mm from the laser fibre at a depth of approximately 30 mm in the liver tissue

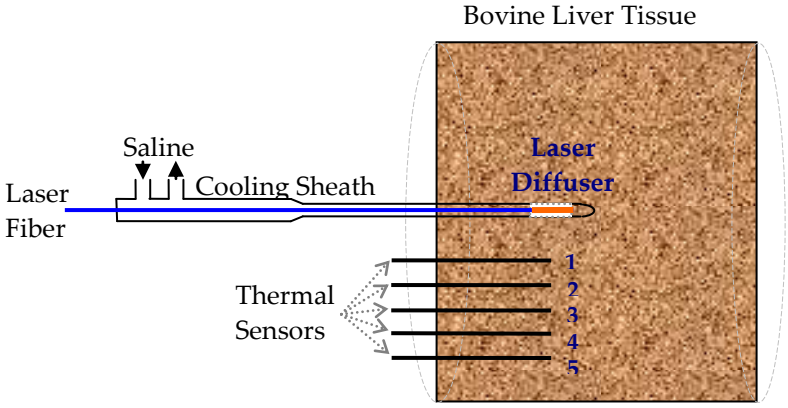

Figure 1

Schematic set up of the bovine liver tissue inside the Plexiglas cylinder. The laser fibre (Nd:YAG, continuous wave of wavelength:1064 nm, diffusing length: 30 mm) with cooling sheath and saline flush was inserted from the top of the cylinder and 5 thermal sensors (NiCr-Ni, diameter: 0.25 mm) were inserted at distances of 10, 15, 20, 25 and 30 mm from the laser fibre.

(Fig. 1). All thermal sensors were connected to a data logger (TopMessage, Delphine Technology, Germany) and real-time temperature was recorded and stored in a personal computer. During each of the four laser heating experiments, the temperature recorded by thermal sensor 1 was referenced to monitor power given to laser when temperature rose from room temperature (18°C) up to a maximum of 85°C.

Before and during each of the four laser heating experiments, each block of liver tissue was examined using multidetector CT (SOMATOM Definition; Siemens AG, Forchheim, Germany). The CT examinations were done in a sequential mode using 120 kVp and 200 mAs in single source mode, a collimation of 12 x 1.2 mm, and a rotation time of 500 ms. The acquired images were adjacently reconstructed with a slice thickness of 1.2 mm, a field of view of 300 mm, and a B31s smooth kernel on a dedicated workstation (Syngo, Siemens AG, Forchheim, Germany). In each CT examination, the tissue was imaged at least 1 time before and 7 times during laser heating at the interval of about 5 min.

The radiation dose was read from the workstation of the CT system for each of the four laser heating experiments. The average dose per CT and per examination during each experiment was calculated.

On the CT images, circular region of interests (ROI) with an area of approximately 100 mm^2 were manually drawn around the tip of each of the five thermal sensors. From each of these five ROIs the average CT number and standard deviation were calculated. A linear regression analysis was performed using all measurement points to determine the dependency of the average CT number on temperature and to derive the CT thermal sensitivity. The accuracy

of the fit was tested by calculating R-square coefficient (R^2). The data were analysed using statistical software (SPSS 16.0; SPSS, Chicago, IL, USA).

Results:

During laser heating, a growing hypodense area on the CT images was observed around the laser source and that area showed an increase as a function of time shown in Fig. 2. The formation of hypodense area was caused by declining in CT numbers at increasing temperatures during laser heating of bovine liver tissue.

The regression analysis showed an inverse linear relation between the average CT number and temperature with -0.65 ±0.05 HU/^{o}C (R^2 = 0.78) (Fig. 3) which is a CT thermal sensitivity for the range of 18^{o}C to 85^{o}C. In the figure 3, above 96% measurement points remained within 95% prediction interval. However, few of measured points were sparsely distributed at higher temperature due to CT noise. The image noise showed an increase from 4 to 20 HU when the temperature of the tissue was increased from room temperature to 85^{o}C.

The radiation dose delivered during each CT acquisition was approximately 15 mGy. Depending on the number of CTs that were made during each of the four laser heating experiments, the dose ranged from 92 mGy (8 CTs) to 231 mGy (15 CTs).

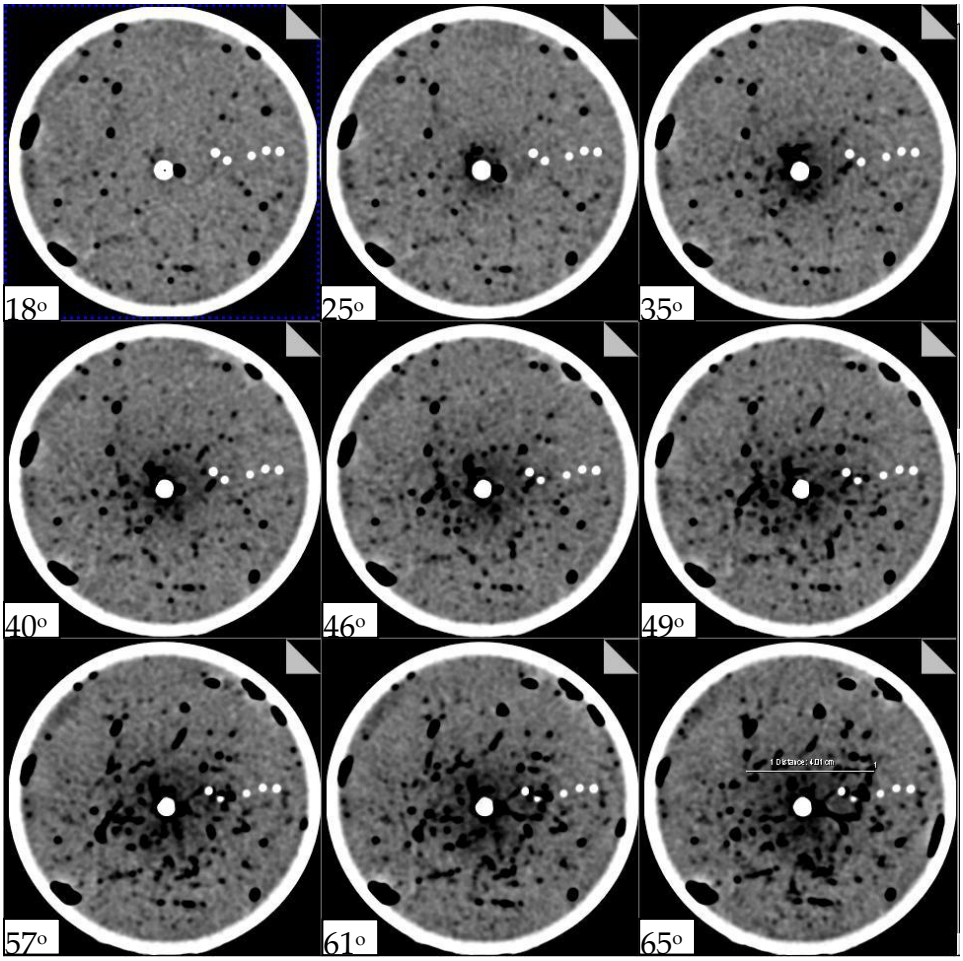

Figure 2

Example of the increase of a hypodense area during LITT in the bovine liver tissue during the LITT procedure. The temperature measured at thermal sensor 1 during LITT was shown in each CT image. The white ring, the central white spot and the five small white spots are the plexiglass cylinder, the laser fiber with cooling system and the thermal sensors respectively. The window/level setting of the images was 100/80.

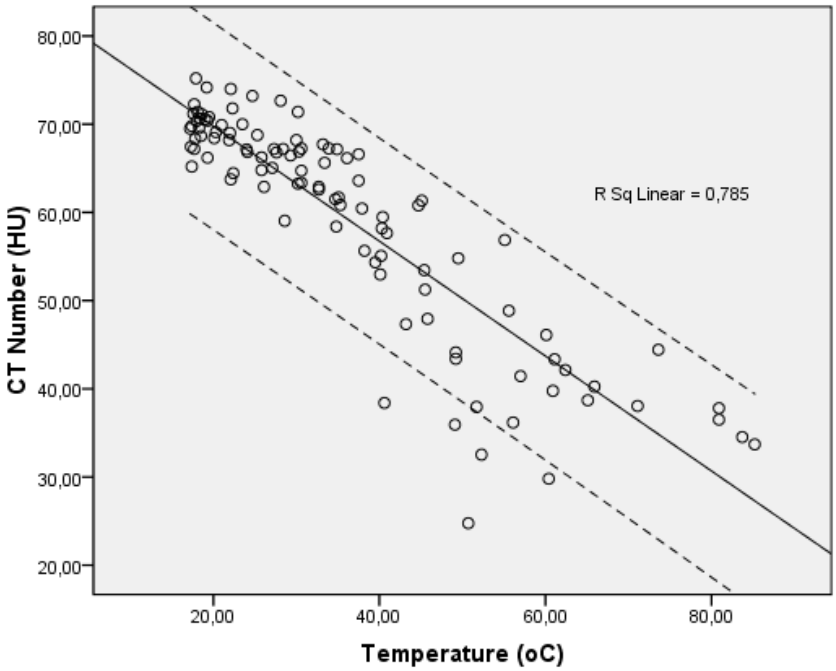

Figure 3

Average CT number in a ROI close to the tip of the five thermal sensors as a function of temperatures. The central line in the graph represents a linear fit and the two dotted lines represent the 95% prediction interval.

Discussion:

In this study, the formation of hypodense area was observed around laser source which ensured the thermal shift of CT number during laser heating of liver tissue. An inverse linear dependency of CT numbers on temperature was found with a CT thermal sensitivity of 0.65±0.05 HU/^{o}C (R^2 = 0.78). The decline in CT numbers depends on temperature change on tissue with its contents. The spatial and temporal distribution of the temperature in the liver was also shown by declining CT numbers on the CT images taken at different time points during laser heating. Thus, the

present study showed in principle that non-invasive CT temperature measurement can be carried out during LITT.

The previous studies [20, 21] showed different values of thermal sensitivity using early CT systems and experimental parameters. Fallone et al [20] measured thermal sensitivity of -0.45 HU/^{o}C where tissue was heated using water bath and imaged using early CT system at 6 sec of rotation time and 15 mm of slice thickness. Jenne et al [21] measured thermal sensitivity of -0.43 HU/^{o}C where tissue was heated using focused ultrasound and imaged using CT system at 1.5 sec of rotation time and 8 mm of slice thickness. Although these studies [20, 21] showed a linear dependency of the CT number on temperature under different experimental parameters, those results can not be retained into the present CT system of below 0.5 sec of rotation time and below 0.3 mm of slice thickness, and heating techniques like laser ablation. The high temporal and spatial resolutions of CT system may provide the accurate temperature information by improving image detail without a significant increase in radiation dose and could assist to improve the temperature resolution. So, this study investigates the potential of current CT for non-invasive thermometry during laser heating.

Although alternative imaging techniques like MRI, US are under investigation for non-invasive temperature measurement during ablation, these techniques have a relatively long acquisition time or a relatively low spatial resolution [12, 17, 22]. Currently, CT systems are available with high spatial and temporal resolution which enables small changes in the treated tissue to be depicted with 3-dimensional isotropic resolution [23]. Nevertheless, radiation dose delivered during imaging could be additional concerns in clinical practice. The radiation delivered during this experiment was under

231 mGy which is far below skin erythema threshold dose of 200 cGy. The dose can be further reduced by limiting the number of scans and by optimising imaging technique.

High temperatures in tissue cause excessive physical forces between molecules, which can lead to various cell destructive processes and to thermal cell damage [24, 25]. It has been shown that thermal damage does not depend on cell size or shape but only on the molecular structure and the strength of chemical bonds in the cell [26]. Therefore, similar effects of thermal damage in different tissue types are expected [24]. Nevertheless, local tissue properties, in particular perfusion, have a significant impact on the extent of thermal damage. Highly perfused tissue and large vessels may act as a heat sink, as laser light is absorbed by erythrocytic heme, and heat is transported from the local tissue area to the peripheral tissue [27]. The effect of perfusion makes native liver parenchyma relatively more resilient to laser induced thermal damage than tumour tissue. In addition, this effect can cause a more asymmetric temperature distribution and a more irregular necrosis zone [28] than the approximately radial symmetric temperature distribution shown in the present study.

There are a few limitations to the present study, which may affect the result. First, the heat distribution might be affected by the presence of the five thermocouples in the necrosis zone. As the heat conduction in the thermocouples was minimised because of the use of mineral-insulated materials a minor influence on the heat distribution during the laser heating experiment is expected because of the presence of the thermocouples. In addition, no interference between laser light and thermocouple sensors was observed distinctive to the optical sensors. Second, although the CT

images were influenced by beam hardening, this effect mainly influenced the CT numbers in the direct vicinity of the cooling sheath. Temperature information in the direct vicinity of the cooling sheath is less necessary than at a larger distance. Therefore, it is estimated that beam hardening only had a minor influence on the present results. Third, the change in CT number after heating was not included in this study. Although, the main concerned is to determine the area of necrosis by detecting the region with temperature above 60^{o}C [9, 29] during heating, further study is necessary to investigate the reversible effect. Fourth, vaporisation during laser heating might hamper the heat conduction and subsequently affects the image quality. In order to reduce this effect a cooling sheath was used [10]. Moreover, because of the relatively small size of the air bubbles and use of relatively high spatial resolution CT system, we estimate that the effect caused by the air bubbles has a minor effect on our study outcome. Finally, the ex-vivo tissue does not resemble an in-vivo tissue situation because of the effects of local physiological processes like perfusion and surrounding heterogeneous structures including bones. Therefore, these effects could increase the noise and cause asymmetric heat distribution [30]. These effects need to be further evaluated in animal studies before implementation in clinical practice is possible.

To the best of our knowledge, the present study is the first study in which liver tissue was heated using laser and in which temperature was measured non-invasively with high-end CT technology. From this study, it is concluded that the non-invasive CT based thermometry during interstitial laser heating is feasible in an ex-vivo bovine liver. The thermal sensitivity may be used to predict temperature development during LITT. Therefore, CT based thermometry may be of potential use during LITT.

References

1. Ferrari FS, Megliola A, et al. Treatment of small HCC through radiofrequency ablation and laser ablation. Comparison of techniques and long-term results. Radiol Med (Torino) 2007; 112:377–393.
2. Fischer K, Gedroyc W, Jolesz FA. Focused ultrasound as a local therapy for liver cancer. Cancer J 2010; 16:118–124.
3. Martin RC, Scoggins CR, McMasters KM. Safety and efficacy of microwave ablation of hepatic tumors: a prospective review of a 5 year experience. Ann Surg Oncol 2010; 17:171–178.
4. Vogl TJ, Eichler K, Straub R et al. Laser-induced thermotherapy of malignant liver tumors: general principals, equipment(s), procedure(s) – side effects, complications and results. Eur J Ultrasound 2001; 13:117–127.
5. Mack MG, Straub R, Eichler K et al. MR-guided laser-induced thermotherapy in recurrent extrahepatic abdominal tumors. Eur Radiol 2001; 11:2041 – 2046
6. Vogl TJ, Straub R, et al. Malignant liver tumors treated with MR imaging-guided laser-induced thermotherapy: experience with complications in 899 patients (2520 lesions). Radiology 2002; 225:367–377.
7. Arienti V, Pretolani S, et al. Complications of laser ablation for hepatocellular carcinoma: a multicenter study. Radiology 2008; 246:947–955.
8. Muralidharan V, Malcontenti-Wilson C, Christophi C. Interstitial laser hyperthermia for colorectal liver metastases: the effect of thermal sensitization and the use of a cylindrical diffuser tip on tumor necrosis. J Clin Laser Med Surg 2002; 20:189–196.
9. Gough-Palmer AL, Gedroyc WM. Laser ablation of hepatocellular carcinoma – A review. World J Gastroenterol 2008; 14:7170–7174.
10. Vogl TJ, Straub R, et al. MR-guided laser-induced thermotherapy (LITT) of liver tumors: experimental and clinical data. Int J Hyperthermia 2004; 20:713–724.
11. Dodd GD, Soulen MC, et al. Minimally invasive treatment for malignant hepatic tumors: at the threshold of a major breakthrough. Radiographics 2000; 20:9–27.
12. Seip R, Ebbini ES. Noninvasive estimation of tissues temperature response to heating fields using diagnostic ultrasound. IEEE Trans Biomed Eng 1995; 42(8):828-839.

13. Weidensteiner C, Quesson B, et al. Real time MR temperature mapping of rabbit liver in vivo during thermal ablation. Magn Reson Med 2003; 50:322–330.
14. Lepitit-Coiffee M, Quesson B, et al. Real time monitoring of radiofrequency ablation of rabbit liver by respiratory gated quantitative temperature MRI. J Magn Reson Imaging 2006; 24:152–159.
15. Wang SS, VanderBrink BA, et al. Microwave radiometric thermometry and its potential applicability to ablative therapy. J Interv Card Electrophysiol 2000; 4(1):295–300.
16. Dick EA, Wragg P, et al. Feasibility of abdomino-pelvic T1-weighted real-time thermal mapping of laser ablation. J Magn Reson Imaging 2003; 17:197–205.
17. De Senneville BD, Roujol S, et al. Motion correction in MR thermometry of abdominal organs: a comparison of the referenceless vs the multibaseline approach. Magn Reson Med 2010; 64: 1373–1381.
18. Homolka P, Gahleitner A, Nowotny R. Temperature dependence of HU values for various water equivalent phantom materials. Phys Med Biol 2002; 47:2917–2923.
19. Bruners P, Levitt E, et al. Multi-slice computed tomography: A tool for non-invasive temperature measurement? Int J Hyperthermia 2010; 26(4):359–365.
20. Fallone BG, Moran PR, et al. Noninvasive thermometry with a clinical x-ray CT scanner. Med Phys 1982; 9(5):715–721.
21. Jenne JW, Bahner M, et al. CT on-line monitoring of HIFU therapy. Proc IEEE Ultrason Symp 1997; 1377–1380.
22. Goldberg SN, Dupuy DE. Image-guided radiofrequency tumor ablation: challenges and opportunities – Part I. J Vasc Interv Radiol 2001; 12:1021–1032.
23. Ueno J, Murase T, et al. Three-dimensional imaging of thoracic diseases with multi-detector row CT. J Med Invest 2004; 51:163–170.
24. Lee RC, Astumian RD. The physicochemical basis for thermal and non-thermal 'burn' injuries. Burns 1996; 22: 509–519.
25. Dewey WC. Failla memorial lecture. The search for critical cellular targets damaged by heat. Radiat Res 1989; 120: 191–204.
26. Breen MS, Breen MB, et al. MRI-guided thermal ablation therapy: Model and parameters estimates to predict cell death from MR thermometry images. Ann Biomed Eng 2007; 35:1391–1403.

27. Whelan WM, Wyman DR, Wilson BC. Investigations of large vessel cooling during interstitial laser heating. Med Phys 1995; 22:105–115.
28. Jiang SC, Zhang XX. Dynamic modelling of photothermal interactions for laser-induced interstitial thermotherapy: parameter sensitivity analysis. Lasers Med Sci 2005; 20:122–131.
29. Goldberg SN, Gazelle GS, Halpern EF, et al. Radiofrequency tissue ablation: importance of local temperature along the electrode tip exposure in determining lesion shape and size. Acad Radiol 1996; 3:212–218.
30. Bydder GM, Kreel L. The temperature dependence of computed tomography attenuation values. J Comput Assist Tomogr 1979; 3:506–510.

CHAPTER 7

General Discussion

The aim of this study was to assess the feasibility of using current CT systems for the optimization of thermal liver ablation. The study concept was validated for a homogeneous medium such as water to an inhomogeneous medium such as bovine liver tissue. Although the specific discussion to the each step in the study was already discussed in previous chapters, the general questions raised during the development of the study will be answered in this chapter.

Background

A noninvasive method to measure the temperature of a solid medium/object without using any probe has many important applications associated with heat therapy such as ablation in medicine. A typical noninvasive method is to monitor temperature distribution during tumor treatment using thermal ablation where the tumor tissue is heated at a temperature above 56^{o}C for a short duration [1]. The temperature of the healthy tissue around the treated tumor, however, should stay below 40^{o}C in order to avoid thermal damage. So, the temperature information acquired during ablation should allow controlling the tumor treatment and should optimize the effectiveness of the treatment method. The currently available invasive methods (e.g. thermocouple, thermistor or optical probes), however, have a limited accuracy [1, 2] and can only be applied to reachable and limited locations. In addition, the invasive methods can also cause morbidity, infection, bleeding and tumor growth along the catheter track. Thus, a noninvasive temperature measurement is desirable and might provide reliable control during the ablation by providing real-time temperature information.

Noninvasive temperature measurements using imaging systems

such as microwave radiometry [3], magnetic resonance imaging (MRI) [4, 5] and ultrasound (US) [6, 7] are currently under investigation. However, it has been shown that these imaging systems are relatively insensitive to temperature changes in moving and refilling organs. Computed Tomography (CT) as a potential candidate for noninvasive temperature measurements during ablation has surprisingly been ignored for the last decades, even though the pioneering work of Fallone et al. (1982) demonstrated that temperature profiles could be visualized on CT images [8]. It has also been shown that CT numbers depend linearly on temperature. However, the calibration of CT for the quantification of temperature information remained a major challenge because of a poor resolution and excessive radiation dose.

Noninvasive thermometry during ablation based on the temperature dependency of CT-numbers is beneficial for several reasons:

(1) There is no need for special ablation equipment because all commercially available ablation systems are compatible with modern CTs compared to MRI where all devices should pass the MR compatibility test. In addition CT does not interfere with Radio Frequency (RF) devices during image acquisition.

(2) CT-guidance for the placement of applicators can be widely used due to the broad availability of CT-scanners with a high spatial resolution, an acceptable soft tissue contrast and the possibility to detect immediate complications such as bleeding.

(3) The additional option to perform CT-based thermometry during ablation would allow for the improvement of the

safety of the procedure by depicting the temperature around vital structures located in the vicinity of the target volume. A three-dimensional visualization of the temperature distribution would also be helpful to decide whether the induced coagulation volume completely covers the target lesion including a safety margin of at least 0.5 cm and thereby reduces the risk for incomplete ablation.

For these reasons, we have assessed the feasibility to use CT for the noninvasive measurement of temperatures during ablation procedures. In the next paragraph the main findings of the experiments we performed will be discussed.

Main Findings

The formation of a hypodense area in the ablated liver region was observed using different heat sources. The hypodense area showed a linear decline of the average CT number as a function of temperature in chapters 2 to 6. The spatial and temporal temperature distribution in the liver could be assessed by obtaining CT images at different time points during the ablation treatment. The present study shows that noninvasive CT temperature measurement during ablation treatment is feasible.

All of the experiments mentioned in chapters 2 to 6 showed that noninvasive assessment of temperature during ablation is feasible. The measured CT thermal sensitivities during the experiments are shown in table below. In addition, the measured CT thermal sensitivity was also used to calculate a color-coded temperature map (shown in chapter 4).

Previous studies [8, 9] showed different values of thermal

sensitivities using early CT systems and different experimental parameters. The results of those studies cannot be correlated with our results because of different experimental set-ups but the concept of linear dependency of CT number during change of temperature is established. The current results are quantitatively close to the desired criteria mentioned by Frich et al [10] for noninvasive thermometry and further clinical implication of this method. Nevertheless, optimising temporal and spatial resolutions of current CT system may improve image quality without a significant increase in radiation dose and could, further, assist in improving the temperature resolution.

Table 1. CT thermal sensitivity for different experimental set-ups.

Chapter #	Tissue type	Energy source	CT thermal sensitivity	Statistical Analysis
2	Ex-vivo; Swine liver	Heated PTFE tube	-0.54 ± 0.03 HU/°C	$R^2 = 0.91$
3	Ex-vivo; Bovine liver	Mono-polar RF	-0.54 ± 0.10 HU/°C	$R^2 = 0.97$
4	Ex-vivo; Bovine liver	Mono-polar RF	-0.60 ± 0.03HU/°C	$R^2 = 0.87$
5	Ex-vivo; Swine liver	Bipolar RF	-0.35 to -0.44 HU/°C	N/A
	In-vivo; Swine liver	Bipolar RF	-0.03 to -0.43 HU/°C	P-value: 0.172 to 0.005
6	Ex-vivo; Bovine liver	Laser	-0.65 ± 0.05 HU/°C	$R^2 = 0.78$

Methodological considerations

The use of different heating techniques, scan parameters and ablated tissues complicates the comparison of our results to previous studies. Previous studies [8, 9] were using either a hot bath or ultrasound to heat the tissue while in our study a hot air polytetrafluoroethylene (PTFE) tube, an RF source and a laser were used to heat the tissue.

One of the main drawbacks for the use of CT for noninvasive measurement of temperature during ablation treatments is the formation of image artifacts. Because of the metal in the ablation needle, large streaking artifacts can be seen in the CT slices which include the needle. The metal artifacts hamper the accurate assessment of CT numbers in the vicinity of the needle and, therefore, make the assessment of accurate temperature information in the ablated region cumbersome. However, it has been argued that accurate temperature information is especially important at the border of the ablated area where the metal artifacts are less pronounced. Nevertheless, special metal artifact reduction algorithms [11] can be used to obtain temperature information in the immediate vicinity of the ablation needle but the CT numbers calculated by these algorithms are not reliable for quantitative evaluation yet [12] and hence cannot be used to obtain reliable temperature information. Therefore, further study is needed to explore the noninvasive measurement of temperature close to ablation needle.

CT scan parameters play a major role in CT image acquisition. Earlier studies [8, 9] were performed with relatively low spatial and temporal resolution, which may have reduced the accuracy of the correlation of the temperature measurement and the CT numbers. Current CT scanners have been further improved for high-quality image by optimising various parameters, particularly temporal resolution and spatial resolution. Recently, Bruners et al. [13] estimated that current CT scanners could realize a temperature resolution of 3 – 5^{o}C. However, a desired temperature resolution [8] of approximately 2^{o}C could not be achieved in the present study due to a CT noise of 6 HU equivalent to ~3^{o}C. Furthermore, CT noise is expected to increase further in in-vivo examinations due to

the presence of inhomogeneous structures and local physiological effects [8]. Therefore, further studies are needed to assess the feasibility of noninvasive temperature assessment with CT during RF ablation of the liver in a clinical setting.

Clinical implications

Criteria for noninvasive thermometry for the monitoring of thermal ablation in clinical use are: a spatial resolution lower than 2 mm (1), an acquisition time less than 30 s (2), and a temperature accuracy better than 2°C (3) [10]. In the present study criteria (1) and (2) were met with a spatial resolution of 1.2 mm and an acquisition time of 500 ms. Although it has been shown that a temperature accuracy of approximately 5°C is feasible with sub-millimeter spatial resolution [13], criterion (3) was not met. However, we expect that the temperature accuracy can be increased by using nonmetallic thermal sensors and improving image quality.

Compared to other imaging techniques such as MRI, CT systems are available with high spatial and temporal resolution which enables small changes in the treated tissue to be depicted with 3-dimensional isotropic resolution [14]. But radiation dose delivered during CT imaging could be an additional concern in clinical practice. For CT temperature assessment, Bruners et al. [13] reported that it is necessary to perform a baseline scan and at least 5 repeated scans to monitor the temperature induced changes in CT numbers. An effective dose of approximately 12 mSv for the entire ablation procedure of one experimental set-up was observed in the present study. This is 8 to 10 mSv more than the 2 to 4 mSv used in a conventional CT scan of the liver. The risk-benefit analysis assessed in chapter 2 showed that the benefit due to the tumor

treatment monitored by CT will surpass the risk due to excessive radiation dose delivered during treatment.

The color-coded temperature map obtained in the present study can be used to derive the thermal dose which is defined as the product of the temperature and the duration of the heat application. Furthermore, this map may be used to calculate the cumulative equivalent minute (CEM) during low heating thermal therapy such as hyperthermia [15]. Hence, a color–coded temperature map could improve the efficiency of thermal therapy by providing real time temperature information of the ablation area.

Future directions

This ablation study was performed in ex-vivo and in-vivo tissues and thermal sensitivity of CT was assessed in 7 different experimental set-ups. The use of CT to monitor temperature distribution was enhanced in the results of all experiments. The outcome of this study will further be improved if the following recommendations are carried out:

i) Metal artifacts: The temperature information close to the metallic ablation device may be less important but it might be important during the treatment of small tumors. Currently available metal artifact reduction algorithms are not clinically reliable to implement for quantitative evaluation because of the lack of clinical validation of those algorithms. Further development of those algorithms will allow revealing the temperature information in the direct vicinity of the metallic ablation device.

ii) Tissue perfusion: The role of tissue perfusion has to be further investigated during in-vivo and clinical studies. The effect occurs due to perfusion during ablation owing to the change of blood volume in the ablation area. In addition, changes of tissue density due to coagulation alter the tissue perfusion which also affects the blood volume during ablation in the ablation area. In an in-vivo ablation, heating first causes vasodilatation but at higher temperature vasoconstriction occurs, and as a consequence the tissue blood volume changes.

iii) Tissue thermal hysteresis: During this study, the key interest was whether CT could show the temperature dependency when tissue temperature became higher than 60^{o}C during heating. It was not investigated whether CT numbers will follow the same temperature dependency during cooling of the tissue. This reversal behavior should be analyzed in further studies. This could establish that the change in CT numbers is due to temperature and not due to ablation related tissue destruction.

iv) Radiation dose: The radiation dose is one of the main concerns in CT thermometry. As mentioned in previous chapters, the radiation dose is within an acceptable range but further research is needed to reduce the dose either by optimizing the scan protocol or by improvement of the imaging system.

v) CT noise: A temperature accuracy of less than 2°C is expected in clinical practice of CT thermometry but the results presented here do not meet this criterion due to noise

in the images, even though CT number thresholds were used. Although it has been shown that a temperature accuracy of approximately 5°C is feasible with sub-millimeter spatial resolution [13], the temperature accuracy can be further increased by improving the CT image quality and using nonmetallic thermal sensors.

A new CT image reconstruction method, called iterative reconstruction (IR), achieves better image quality by reduction of image noise and radiation dose, and improvement of diagnostic confidence than the conventional filter-back projection (FBP) algorithm_in CT examination [16] IR algorithm is performed in three steps: creation of artificial raw data by forward projection of an estimated volumetric image, comparison of the artificial raw data with the measured raw data, and finally the back projection of the corrected artificial raw data to the current volumetric image. This IR is completed either after a fixed number of iterations or after reaching a given criterion. Although noise in CT images is intermingled with the sharpness of the images, IR uses noise modeling techniques considering noise propagation sources without compromising the sharpness of the images. Different models [17] of IR are available such as sinogram affirmed iterative reconstruction (SAFIRE) [16], adaptive statistical iterative reconstruction (ASIR) [18]. Compared to FBP, IR increases the image quality and maintains the diagnostic accuracy at a reduced radiation dose. So implementation of IR could reduce the noise during non-invasive CT thermometry and might therefore increase the temperature accuracy from the currently offered accuracy of 5°C. In addition, the radiation dose will be significantly decreased by using IR.

The concepts presented in this study can be of potential use for a noninvasive method to monitor temperature during ablation using CT. Furthermore, this method should be able to meet the required criteria [10] by considering the recommendations mentioned above as the future research work. Consequently, this concept will then be realized in clinical setting for noninvasive real-time temperature measurements.

Conclusions

It can be concluded from present study that CT-based noninvasive thermometry is feasible during ablation. The spatial and temporal temperature distribution shown in the real-time temperature map could enhance the efficiency of the treatment. The negative correlation between tissue temperature and CT number in an ex-vivo and in-vivo model should be further explored for its implementation in clinical settings. Thus, the ability of CT for noninvasive thermometry may be extended from the established CT-based treatment planning of ablation to CT-based monitoring of the thermal therapy during ablation.

References

1. Goldberg SN and Dupuy DE. Image radiofrequency tumor ablation: challenges and opportunities – part 1. J Vasc Interv Eadiol 2001; 12:1021 – 1032.
2. Van der Zee J, Peer-Valstar JN, et al. Practical limitation of interstitial thermometry during deep hyperthermia. Int J Radiat Oncol Biol Phys 1998; 40:1205 – 1212.
3. Wang SS, VanderBrink BA, et al. Microwave radiometric thermometry andits potential applicability to ablative therapy. J Interv Card Electrophysiol 2000; 4(1): 295 – 300.

4. Weidensteiner C, Quesson B, et al. Real time MR temperature mapping of rabbit liver in vivo during thermal ablation. Magnetic resonance in Medicine. 2003; 50:322 – 330.
5. Lepetit-Coiffe M, Quesson B, et al. Real time monitoring of radiofrequency ablation of rabbit liver by respiratory gated quantitative temperature MRI. J of Magnetic Resonance Imaging. 2006; 24:152 – 159.
6. Arthur RM, Straube WL, et al. Noninvasive temperature estimation based on the energy of backscattered ultrasound. Med Phys 2003; 30:1021-1029.
7. Seip R, Ebbini ES. Noninvasive estimation of tissues temperature response to heating fields using diagnostic ultrasound. IEEE Trans. Biomed. Eng. 1995; 42(8).
8. Fallone BG, Moran PR, et al. Noninvasive thermometry with a clinical x-ray CT scanner. Med Phys 1982; 9(5):715-721.
9. Jenne JW, Bahner M, et al. CT on-line monitoring of HIFU therapy. Proc IEEE Ultrason Symp 1997; 1377-1380.
10. Frich L. Non-invasive thermometry for monitoring hepatic radiofrequency ablation. Minim Invasive Ther 2006: 15:18-25.
11. Barett JF, Keat N. Artifacts in CT: Recognition and avoidance. Radiographics 2004; 38:1679-1691.
12. VeldKamp WJH, Joemai RMS, van der Molen Aj, et al. Development and validation of segmentation and interpolation techniques in sonograms for metal artifact suppression in CT. Med Phys 2010; 37: 620-628.
13. Bruners P, Levitt E, et al. Multi-slice computed tomography: A tool for non-invasive temperature measurement? Int J Hyperthermia 2010; 26: 359-365.
14. Ueno J, Murase T, et al. Three-dimensional imaging of thoracic diseases with multi-detector row CT. J Med Invest 2004; 51:163-170.
15. Mertyna P, Dewhirst MW, et al. Radiofrequency ablation: The effect of distance and baseline temperature on thermal dose required for coagulation. Int J Hyperthermia 2008; 24:550-559.
16. Kalra MK, Woisetschlaeger M, et al. Radiation dose reduction with sonogram affirmed iterative reconstruction technique for abdominal computed tomography. J Comput Assist Tomogr 2012; 36:339-346.
17. Beister M, Kolditz D, Kalender WA. Iterative reconstruction methods in X-ray CT. Physica Medica 2012; 28:94-108.
18. Mitsumori LM, Shuman WP, et al. Adaptive statistical iterative reconstruction versus filtered back projection in the same patient: 64 channel

liver CT image quality and patient radiation dose. Eur Radiol 2012; 22:138-143.

CHAPTER 8

Summary

Thermal ablation is a widely used method to treat malignant tumors by generating a high tissue temperature. Thermal ablation is performed using various techniques such as radiofrequency (RF), laser and ultrasound (US) to deliver heat. The irreversible cell damage, called thermal coagulation necrosis, occurs during ablation when tissue is exposed to a temperature of 55 to 57^{o}C. Therefore, the key aim of ablation is to maintain the temperature at 55 to 57^{o}C in the entire target tumor volume while keeping the temperature of the nearest vital structures below 40^{o}C. Despite much effort to achieve this aim, thermal ablation is still facing challenges such as how to deal with irregular tumor volumes, variable tissue perfusion and partial treatment of the target tumor volume. Most of these challenges are manageable if tissue temperature at the tumor volume is monitored during the ablation. Invasive methods using interstitial thermal sensors can be used to monitor this tissue temperature. However, these invasive methods can cause several complications such as bleeding, infection and tumor growth along the catheter in invasive methods. Therefore, non-invasive imaging techniques such as magnetic resonance imaging (MRI), ultrasound (US) and computed tomography (CT) are getting additional interest during ablation. The present study was focused on using CT to obtain real-time temperature information during ablation.

CT is a readily available imaging technique in hospitals and has an excellent spatial and temporal image resolution. The images acquired from CT are represented by CT numbers (given in Hounsfield units, HU) which are defined basically by the photon intensity of x-ray that traversed through the tissue. The CT number is directly proportional to the electron density of the tissue. Temperature changes in the tissue cause a change in tissue density because of the thermal expansion which leads to a change in

electron density. Therefore, the CT numbers in the CT images are sensitive to temperature changes, also called CT thermal sensitivity. Despite a few early studies, this basic principle of CT thermal sensitivity has so far not been further explored due to technical limitations of the early stage CT systems. Recently, new generation CT systems have improved in various aspects, such as spatial and temporal resolution. Hence, the potential of current CT systems can be investigated to determine the CT thermal sensitivity, and the potential use in non-invasive thermometry can be explored.

In this thesis, a feasibility study for non-invasive CT thermometry using different ablation techniques in ex-vivo and in-vivo samples was performed. During thermal ablation, the temperature in the samples was raised either from room temperature for the ex-vivo experiments, or from body temperature for the in-vivo experiments, to nearly 90^{o}C. Changes in CT numbers in the heated area were observed in all experiments. The thermal sensitivity was quantified in the different experiments.

In **chapter 2**, the thermal sensitivity of CT was assessed in ex-vivo swine liver tissue samples. The tissue samples were heated with a hot air tube of poly-tetra-fluoro-ethene. The temperatures at five locations around the tube in the tissue samples were measured using calibrated metal thermocouples. A multi-slice CT scanner was used to acquire images before and during heating of the tissue samples. An increase in temperature of the tissue close to the tube was observed as a hypodense area in CT image caused by a change in CT numbers. In addition, the hypodense area showed that the heat distribution was nearly symmetrical around the tube and that this area increased during heating. Gas pockets were formed close to the tube at elevated temperatures. To minimize the influence of

gas pockets in the assessment, a lower threshold of 0±4.9 HU was determined. Also, image artifacts due to the metallic RF ablation needle and thermocouple probes were minimized by an upper threshold of 70±6.8 HU. Using these thresholds, a thermal sensitivity of -0.54±0.03 HU/^{o}C (R^2=0.91) was determined for the temperature range of 20 ^{o}C to 90^{o}C. The effective radiation dose was approximately 12 mSv. Although, this effective dose was slightly larger than a default scan dose of 8 mSv, the benefit of the tumor treatment under CT thermometry could exceed the risk of radiation. The effective dose can be reduced by limiting the number of scans or by optimizing the imaging acquisition technique.

In **chapter 3,** the thermal sensitivity was investigated for bovine liver tissue samples which were heated using multi-tined RF ablation needles. During heating, CT images were acquired and synchronously the temperature was measured using thermocouples. This study showed that the spatial temperature distribution in the tissue is a function of heating time. The CT thermal sensitivity of bovine liver tissue was -0.54±0.10HU/^{o}C (R^2=0.97). From this experiment we conclude that a new generation CT scanner can be calibrated to assess the temperature distribution during ablation.

In **chapter 4**, non-invasive CT thermometry was assessed during RF ablation of bovine liver. Bovine liver tissue samples were placed in a perspex cylinder and scanned using CT. The thermal sensitivity was calculated from the correlation between CT numbers in the CT images and the measured temperatures as indicated by thermocouples. The thermal sensitivity was -0.60 ± 0.026HU/^{o}C (R^2=0.87). In addition, the thermal sensitivity was translated into a color coded temperature map which showed the temperature

distribution during the ablation. The temperature map showed a relatively symmetric temperature distribution in the bovine liver.

In **chapter 5**, CT-based temperature monitoring during hepatic RF ablation in four in-vivo porcine models was assessed. Three optical temperature probes were inserted to monitor the temperature at fixed distances from a bipolar RF needle. A regression analysis, to analyze the relationship between CT numbers and temperature, showed a negative regression coefficient, ranging from -0.025 (p value: 0.1721) to -0.432 (p value: 0.0050). This in-vivo study showed that CT is able to depict temperatures during RF ablation.

In **chapter 6**, the feasibility of CT-based thermometry during interstitial laser heating in a bovine liver was assessed. Four freshly excised cylindrical blocks of bovine tissue were heated using a continuous laser. All tissues were imaged using CT during laser heating, and temperatures were simultaneously measured with 5 calibrated thermal sensors. A regression analysis showed a negative linear dependency between local temperatures and area averaged CT numbers. The thermal sensitivity was -0.65 ±0.048 HU/^{o}C (R^2 = 0.75) for the temperature range of 18 to 85^{o}C. The noise was increased from 4 to 20 HU when the temperature of the tissue increased from room temperature to 85^{o}C. Despite this relatively large image noise, it was shown that CT-based thermometry is feasible during interstitial laser heating.

In conclusion, the results described in this thesis show an inverse linear dependency between local temperatures and area-averaged CT numbers during heating of ex-vivo and in-vivo tissue models. All criteria, apart from a criterion about the temperature accuracy, for non-invasive thermometry (Frich et al. [2006]) were

accomplished using CT during this study. More in-vivo studies will be needed to further improve the concept of non-invasive CT thermometry. As a result, this concept could be implemented into clinical practice for the treatment of tumors with real-time CT temperature monitoring.

HOOFDSTUK 8

Samenvatting

Thermische ablatie is een veel gebruikte methode om kwaadaardige tumoren te behandelen. Hierbij wordt het weefsel tot een hoge temperatuur verwarmd met behulp van radiofrequente, laser of ultrasone technieken. De verwarming tot hoge temperaturen leidt tot onomkeerbare beschadiging van cellen (thermische coagulatie necrose), die optreedt wanneer weefsel wordt blootgesteld aan een temperatuur van 55-57^{o}C. Het is belangrijk om de temperatuur in het gehele doel tumorvolume op deze temperatuur te brengen, terwijl de temperatuur van het omliggende gezonde weefsel onder de 40^{o}C blijft. Hoewel er veel moeite is gedaan om dit doel te bereiken, heeft thermische ablatie nog steeds een aantal uitdagingen, zoals de behandeling van onregelmatige tumorvolumes, variabele weefselperfusie en gedeeltelijke behandeling van het tumorvolume. De meeste van deze uitdagingen zijn goed beheersbaar als de weefseltemperatuur in het tumorvolume bewaakt wordt tijdens de ablatie. Invasieve methoden maken gebruik van interstitiële thermische sensors om de weefseltemperatuur te controleren. Dit kan echter aanleiding geven tot verschillende complicaties zoals bloedingen, infectie en tumorgroei langs de katheter. Daarom wordt nu onderzoek gedaan naar niet-invasieve technieken zoals magnetic resonance imaging (MRI), echografie (US) en computertomografie (CT). Het doel van deze studie was om met behulp van CT real-time temperatuur informatie te verkrijgen tijdens de ablatie.

CT is een algemeen beschikbare beeldvormende techniek in ziekenhuizen en heeft een uitstekende ruimtelijke en temporele beeldresolutie. De beelden verkregen met CT worden gerepresenteerd in CT-getallen (in Hounsfield eenheden, HU), die in principe zijn gedefinieerd door de intensiteit van de röntgenbundel die het weefsel doorkruist. Het CT- getal is

evenredig met de elektronendichtheid van het weefsel. Temperatuursveranderingen in het weefsel geven aanleiding tot een verandering in de weefseldichtheid ten gevolge van thermische uitzetting, wat weer aanleiding geeft tot een verandering in de elektronendichtheid. CT-getallen zijn daarom gevoelig voor temperatuurveranderingen, ook wel CT warmtegevoeligheid genoemd. Hoewel er enkele vroege studies naar CT warmtegevoeligheid gedaan zijn, is het niet verder onderzocht vanwegen te veel technische beperking. Met de komst van de nieuwe generaties CT-systemen zijn onder andere de spatiële en temporele resolutie sterk verbeterd. Daarom kunnen deze CT-systemen nu verder worden onderzocht om de CT warmtegevoeligheid te bepalen, en het potentieel gebruik hiervan voor niet-invasieve temperatuurmetingen.

In dit proefschrift is een haalbaarheidsstudie uitgevoerd naar niet-invasieve CT thermometrie met behulp van verschillende ablatie technieken in ex-vivo en in-vivo monsters. Gedurende de thermische ablatie, werd de temperatuur in de monsters verhoogd van kamertemperatuur voor ex-vivo experimenten of lichaamstemperatuur van de in vivo experimenten naar bijna 90^{o}C. Veranderingen in CT-getallen in het verhitte gebied werden waargenomen in alle experimenten en daaruit werd de warmtegevoeligheid van de CT-getallen bepaald.

In **hoofdstuk 2** werd de warmtegevoeligheid van CT bepaald in ex-vivo monsters van leverweefsel van varkens. De monsters werden verhit met hete lucht in een buis van poly-tetra-fluor-etheen. De temperatuur in de monsters op vijf locaties rond de buis werd gemeten met geijkte metalen thermokoppels. De monsters werden gescand met een multislice CT scanner voor en tijdens het

verwarmen. Nabij de buis werd een toename in de temperatuur van het weefsel waargenomen als hypodense gebied in het CT beeld. Het hypodense gebied bleek een nagenoeg symmetrische warmteverdeling te hebben rond de buis en waarbij de oppervlakte van het gebied toenam tijdens het opwarmen. Gasbellen werden in de buurt van de buis gevormd verhoogde temperaturen. Bovendien werden gasbellen gevormd in het weefsel bij hogere temperaturen. Om de invloed van de gasbellen op de analyse van de warmtegevoeligheid van de CT-getallen te beperken, werd een ondergrens voor de analyse van de CT-data bepaald van 0 ± 4.9 HU. Ook werden beeld artefacten als gevolg van de metalen radio-frequente ablatienaald en de thermokoppel temperatuursensoren tot een minimum beperkt door middel van een bovengrens van 70 ± 6.8 HU. Met behulp van deze onder- en bovengrens werd een warmtegevoeligheid bepaald van -0.54 ± 0.03 HU/^{o}C (R^2 = 0.91) voor het temperatuurbereik van 20 tot 90^{o}C. De effectieve stralingsdosis was ongeveer 12 mSv. Hoewel deze effectieve dosis groter is dan een standaard dosis van 8 mSv, weegt het voordeel van tumorbehandeling op tegen het risico van ioniserende straling. De effectieve dosis kan nog verder worden verminderd door het aantal scans te verminderen of door middel van optimalisatie van de beeldvormende techniek.

In **hoofdstuk 3** is de warmtegevoeligheid onderzocht voor monsters van runderlevers te verwarmen met behulp van een meerdraads radiofrequente ablatienaald. Tijdens het verwarmen werd een state-of-the-art CT gemaakt en werd de temperatuur gemeten met behulp van thermokoppels. Hieruit bleek dat de ruimtelijke temperatuurverdeling in het weefsel afhankelijk is van de mate van verwarming. De CT warmtegevoeligheid van runderlever werd bepaald op -0.54 ± 0.10 HU/^{o}C (R^2 = 0.97). Uit dit

experiment kunnen we concluderen dat een state-of-the-art CT-scanner zo kan worden gekalibreerd dat de temperatuurverdeling tijdens de ablatie gemeten kan worden.

In **hoofdstuk 4,** wordt het gebruik van niet-invasieve CT thermometrie beoordeeld tijdens radiofrequente ablatie van schapenlevers. Monsters van schapenlever werden in een perspex cilinder geplaatst en gescand met CT. De warmtegevoeligheid werd berekend uit de correlatie tussen CT-getallen en de temperatuur zoals gemeten door de thermokoppels. De warmtegevoeligheid was -0.60 ± 0.03 HU/^{o}C (R^2 = 0.87). Bovendien werd op basis van gemeten warmtegevoeligheid een afbeelding gemaakt van de temperatuurverdeling tijdens de ablatie. De temperatuurverdeling was relatief symmetrisch rondom de ablatienaald.

In **hoofdstuk 5,** wordt het gebruik van niet-invasieve CT thermometrie in-vivo beoordeeld tijdens de radiofrequente leverablatie bij varkens. Op een vaste afstand van een bipolaire radiofrequente naald werden bij de varkens drie optische temperatuursensoren ingebracht. Een regressie analyse van de relatie tussen het CT-getal en de temperatuur leverde een negatieve regressiecoëfficiënt tussen -0.025 (p-waarde: 0.17) tot -0.432 (p-waarde: 0.005). Dit in-vivo onderzoek toont aan dat met behulp van CT temperatuur gemeten kan worden in levende modellen tijdens RF ablatie van de lever.

In **hoofdstuk 6** wordt de haalbaarheid van niet-invasieve CT thermometrie tijdens interstitiële laserverwarming in een runderlever bestudeerd. Vier vers uitgesneden cilindrische blokken runderlever werden verwarmd met behulp van een continue laser. De weefsels werden tijdens de verwarming met de laser

afgebeeld met CT, terwijl de temperatuur werd gemeten met 5 gekalibreerde warmtesensoren. Een regressie analyse gaf een negatief lineaire afhankelijkheid van de gemiddelde CT-getallen en de temperatuur. De thermische gevoeligheid bedroeg -0.65 ± 0.048 HU/^{o}C (R^2 = 0.75) voor het temperatuurbereik van 18 tot 85 ^{o}C. Het ruisniveau steeg van 4 naar 20 HU wanneer de temperatuur van het weefsel verhoogd werd van kamertemperatuur tot 85^{o}C. Ondanks dit relatief hoge ruisniveau werd aangetoond dat temperatuurmetingen met CT haalbaar zijn gedurende interstitiële laserverwarming.

De resultaten beschreven in dit proefschrift laten een negatief lineaire afhankelijkheid zien tussen de lokale temperatuur en oppervlakte-gemiddelde CT-getallen tijdens het verwarmen van ex-vivo en in-vivo lever weefsels. Aan alle gestelde criteria voor niet-invasieve temperatuurmeting (Frich et al. [2006]) werd voldaan, met uitzondering van de temperatuur nauwkeurigheid. Meer in-vivo studies zijn nodig om een verdere verbetering van het concept van non-invasieve CT thermometrie te kunnen bewerkstelligen. Hierdoor is het wellicht mogelijk om dit concept in de klinische praktijk toe te passen voor de ablatie van tumoren en gelijktijdige temperatuurcontrole met behulp van CT.

APPENDICES

Acknowledgement

List of Publications

About the Author

Acknowledgement

At the moment I am about to get my PhD title, I would like to take this opportunity to thank everybody who has contributed at the different stages of the PhD work.

Very sincere thanks go to my supervisors Prof M Oudkerk from the Radiology department at University Medical Center Groningen (UMCG), The Netherlands and Dr. Thomas Flohr at Siemens AG Healthcare, Germany. I would not have been able to carry out the PhD without their constant support and their guidelines.

I thank Dr. Bernhard Schmidt from the CT group at Siemens AG Healthcare in Forchheim, Germany for enabling me to start the PhD and for establishing the collaboration with UMCG and with RWTH University Hospital. Dr. Schmidt has made it possible for me to perform experimental understanding throughout the fruitful stays at the Forchheim site of Siemens AG Healthcare. Especially, I would like to thank Dr. Marcel Greuter for continuously pushing me in the right directions and for four years work in a great environment. Dr. Greuter has not just been a great co-supervisor throughout my PhD work; he has also become a good friend on and off the road. Without his support, this work would have been impossible. Both deserve special thanks for always keeping their doors open in order to discuss the work with great enthusiasm.

My sincere thanks go to my friend and colleague at the Radiology department of UMCG which made it possible to finish my PhD work, here. I would like to thank in particular WGJ Tukker, Dr. KP de Jong and Prof. Dr. EJ van der Jagt. Thanks also to Dr. PMA van Ooijen, who improved my research interest in biomedical

technology and facilitated to link up with Siemens AG Healthcare. Furthermore, I would like to thank Dr. EJK Noah for her sagacious suggestions and constructive criticism to my manuscript and hope to receive her expert comments in the future also.

I take this opportunity to thank Prof. AH Mahnken at the University Hospital, RWTH Aachen University, Germany for animal experiment. I also thanks to Dr. Philipp Bruners, Tobias Penzkoffer from the same hospital. In addition, I would like to thanks to Dr. JHGM Klasessens, Prof. R van Hillegersberg at University Medical Center Utrecht, The Netherlands for the laser experiment.

Also very special thanks to all the friends and colleagues at the Division of CT Engineering (Physics and Applications) of Siemens AG Healthcare for their support during PhD work and in particular to Peter Grininger for technical support.

I would like to thank the members of the reading committee, Prof. dr. ir. CH Slump, Prof. dr. EJ van der Jagt and Prof. dr. JE Wildberger for your critical reading and precious time.

Last but not least, I thank my parents and family for their love and great support throughout my long, maybe unfinished journey through education and science.

Groningen, August 2012

List of Publications

Pandeya GD, Greuter MJW, Schmidt B, Flohr T, Oudkerk M. Assessment of thermal sensitivity of computed tomography during heating of liver: an ex-vivo study. *British Journal of Radiology* 2012; 85:e661-e665

Pandeya GD, Bruners P, Levit E, Roesch E, Penzkofer T, Isfort P, Schmidt B, Greuter MJW, Oudkerk M, Schmitz-Rode T, Kuhl CK and Mahnken AH. CT-based temperature monitoring during hepatic RF-ablation: feasibility in an animal model. *International Journal of Hyperthermia 2012; 28:55 – 61*

Pandeya GD, Greuter MJW, de Jong KP, Schmidt B, Flohr T and Oudkerk M. Feasibility of non-invasive temperature assessment during RF liver ablation on CT. *Journal of Computer Assisted Tomography 2011;* 35:356–360

Pandeya GD, Klaessens JHGM, Greuter MJW and Schmidt B, Flohr T, van Hillegersberg R, Oudkerk M. Feasibility of computed tomography based thermometry during interstitial laser heating in bovine liver. *European Radiology 2011*; 21:1733 – 1738

Pandeya GD, Greuter MJW, Schmidt B, Flohr T, Oudkerk M. Calibration of temperature measurements with CT for ablation of liver tissue, *Proc. SPIE-Medical Imaging 2010*; 7625

Conference Presentations

Pandeya GD, Greuter MJW, Schmidt B, Flohr T, Oudkerk M. Non-invasive temperature mapping by CT during liver ablation: feasibility in vitro. *CIRSE 2009, Lisbon, Portugal (Oral Presentation)*

Pandeya GD, Greuter MJW, Bruners P, Schmidt B, Flohr T, Mahnken A, Oudkerk M. Feasibility of non-invasive thermometry during radio-frequency ablation of in-vivo swine liver using computed tomography. *GUIDE 2010, Groningen, The Netherlands (poster presentation)*

Pandeya GD, Greuter MJW, Schmidt B, Flohr T, Oudkerk M. Calibration of temperature measurements with CT for ablation of liver tissue. *SPIE-Medical Imaging 2010, San Diego, USA (Oral Presentation)*

Pandeya GD, Greuter MJW, Bruners P, Schmidt B, Flohr T, Oudkerk M, Mahnken AH. Noninvasive thermometry for radiofrequency ablation of the liver using computed tomography, an in-vivo animal study. *CARS 2010, Geneva, Switzerland (Oral Presentation)*

Pandeya GD, Greuter MJW, Bruners P, Schmidt B, Mahnken AH, Oudkerk M, Flohr T. Feasibility of noninvasive thermometry during radiofrequency ablation of in-vivo Swine liver using Computed Tomography. *RSNA 2010, Chicago, USA (Oral Presentation)*

About the Author

Ganga Pandeya was born on September 21, 1974 in Harmichaur, Nepal. He was raised together with his 3 brothers in the river valley of the high hills in Nepal. After graduation from secondary school, he joined the Tribhuvan University in Tansen, Nepal in 1992, where he obtained his Bachelors' degree in Science. He continued his studies in Science with major Physics from Tribhuvan University. After receiving his Masters' degree in 1998, this same university offered him to stay as a teaching faculty member.

Ganga lectured for undergraduate students on diverse subjects of physics in Tribhuvan University during five years. As a university lecturer of physics, he followed the theoretical part of modern physics which mostly deals with modern technology. This little insight of modern technology steered his interest towards the field of medical technology.

In 2002, he got an opportunity to attend an intensive course at the European School of Medical Physics, France, where his interest deepened into the field of medical technology. In 2004, he got admission for obtaining his Masters' degree in Applied Physics with a major in Biomedical Technology at the University of Groningen, The Netherlands. He was also selected for the Netherlands Fellowship Program, funded by the Dutch Ministry for Foreign Affairs. His Masters' degree thesis was entitled "Coronary Atherosclerotic Plaque Visualization and Quantification in 64-slice Multi Detector Computed Tomography and Direct Comparison with Intravascular Ultrasound results". He completed his internship at Siemens AG Healthcare, Forchheim, Germany.

After obtaining this second Masters' degree in 2006, he started working as a PhD student at the Department of Radiology of the University Medical Center of Groningen, The Netherlands with the financial support of Siemens AG Healthcare, Germany. He was supervised by Prof. M. Oudkerk and Dr. M.J.W. Greuter. His research was associated with a non-invasive method to monitor liver tumor ablation using computed tomography.

Currently, Ganga lives in Canada since 2010 with his wife – Bal, a daughter – Anshu and a son – Aswin. Ganga is actively involved in the product development research for the treatment of prostate cancer using ultrasound at Sunnybrook Research Institute, University of Toronto, Canada as a Post-Doctoral Fellow.